# Planetary Accretion Models and the Mineralogy of Planetary Interiors


Dan Frost & Dave Rubie – *Bayerisches Geoinstitut*

John Hernlund – *Earth-Life Science Institute, Institute of TechnologyTokyo*

Alessandro Morbidelli & Seth Jacobson – *Observatoire de la Cote d'Azur, Nice, France*

Rebecca Fischer & Andy Campbell – *University of Chicago*

# Structure and dynamics of Earth-like planets

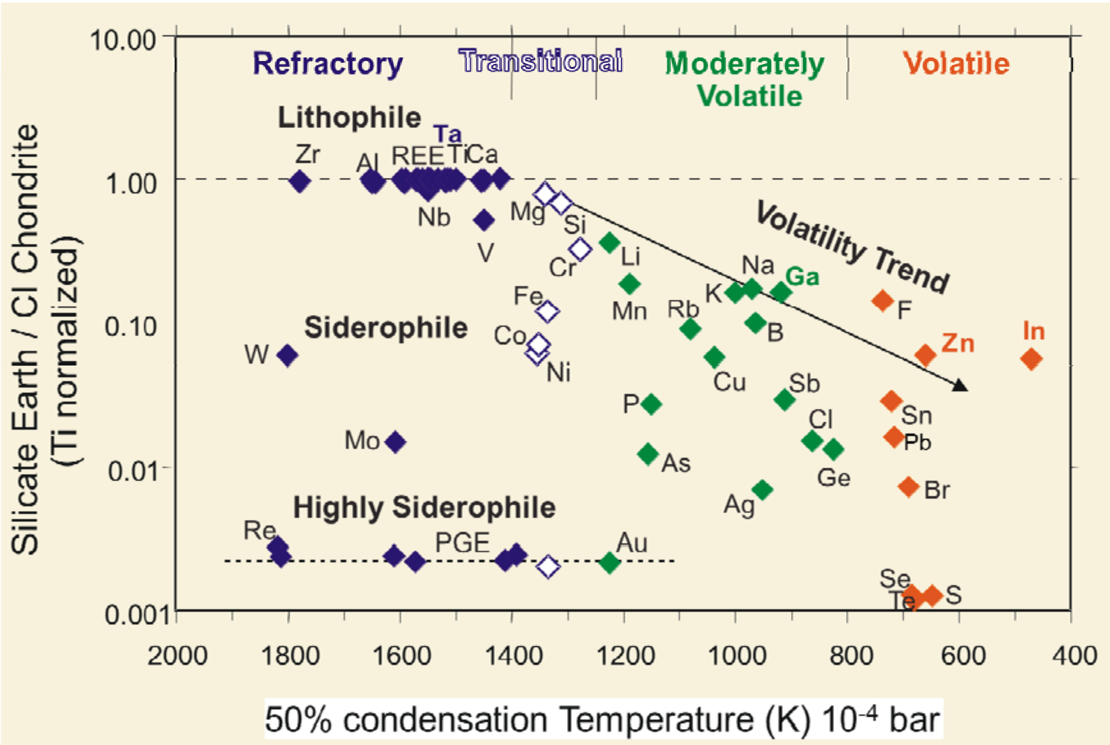


Model incorporates:-

-Partitioning of siderophile elements

-Dynamic/ astrophysical constraints on accretion processes

-Constrain success of the model by comparison with Earth mantle composition

- Provide robust indicators for ranges of plausible conditions

# Heterogeneous Formation of Earth and Moon

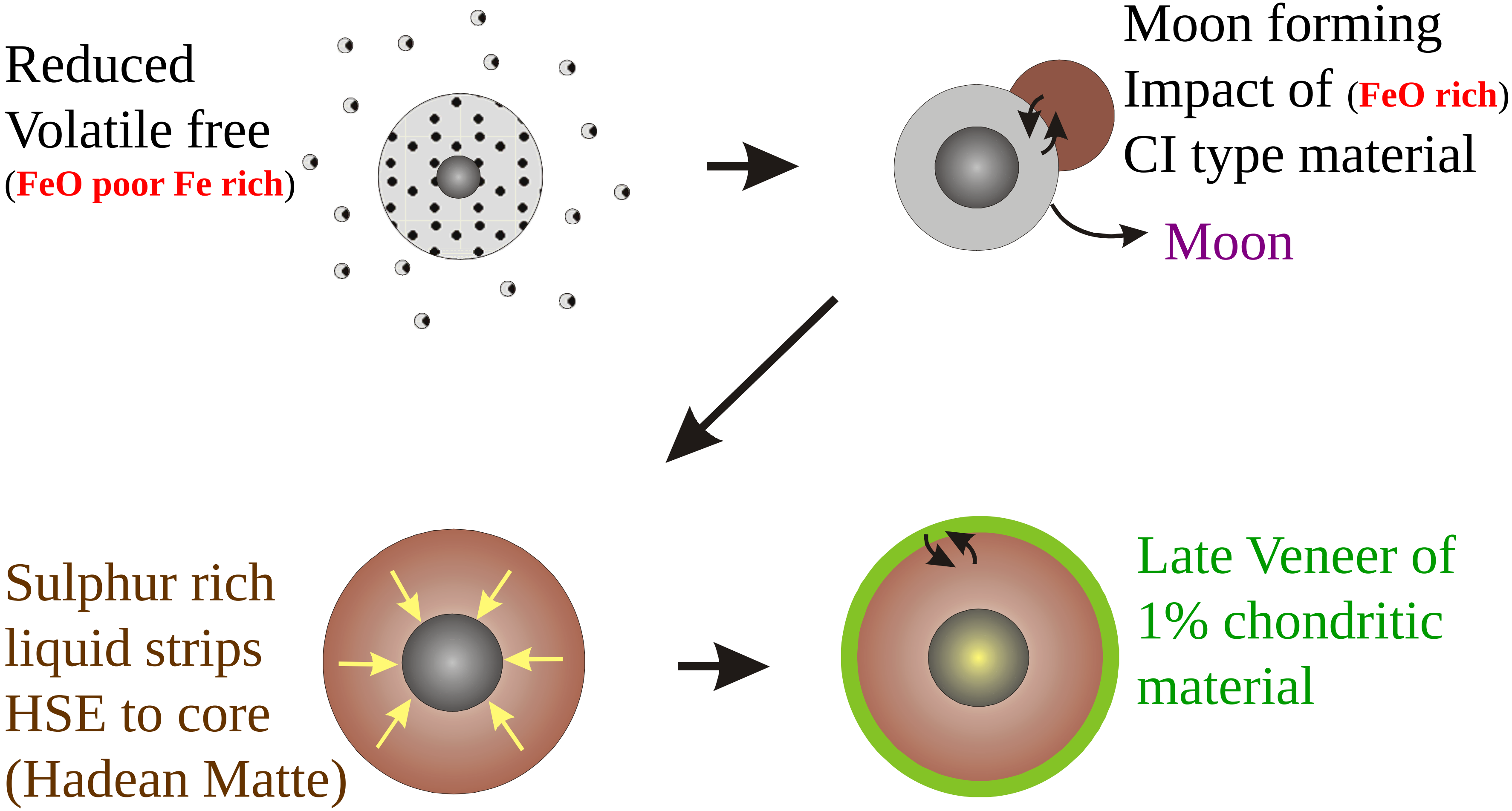


Complicated- can it really be tested?

O'Neill (1991) GCA 55, 1159.

# Homogeneous accretion: Metal segregation at the base of a deep magma ocean

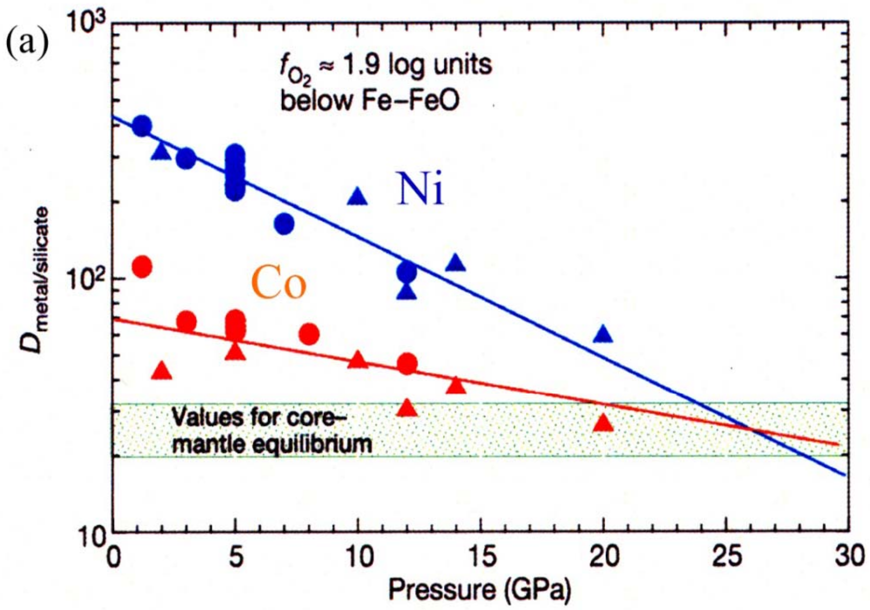


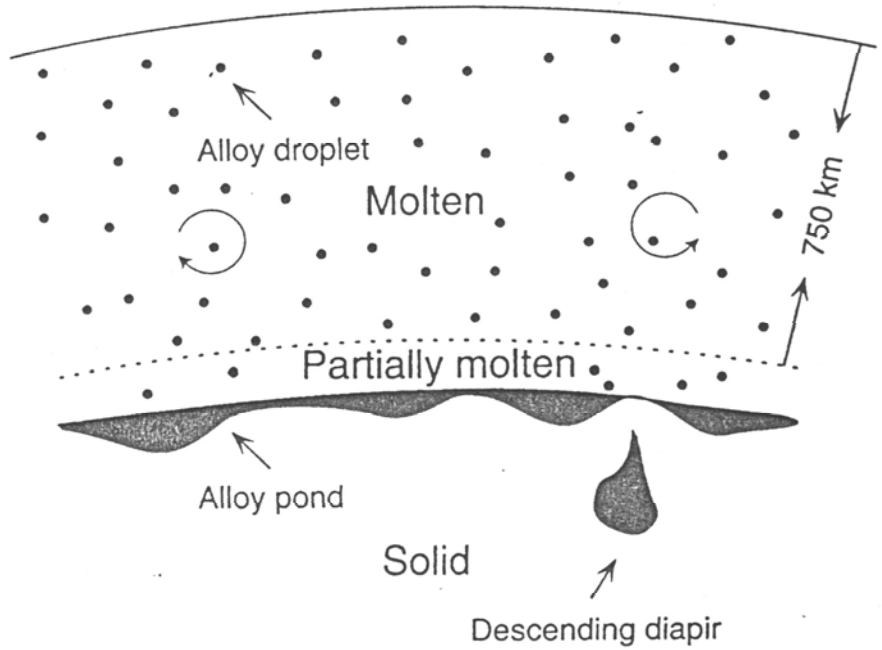


Constrain a single set of P,T and $fo_2$ for core formation

(Li & Agee, 1996; Righter & Drake 1997)

# Model of continuous core formation with step-wise increases in $fo_2$

(Wade & Wood, 2005)

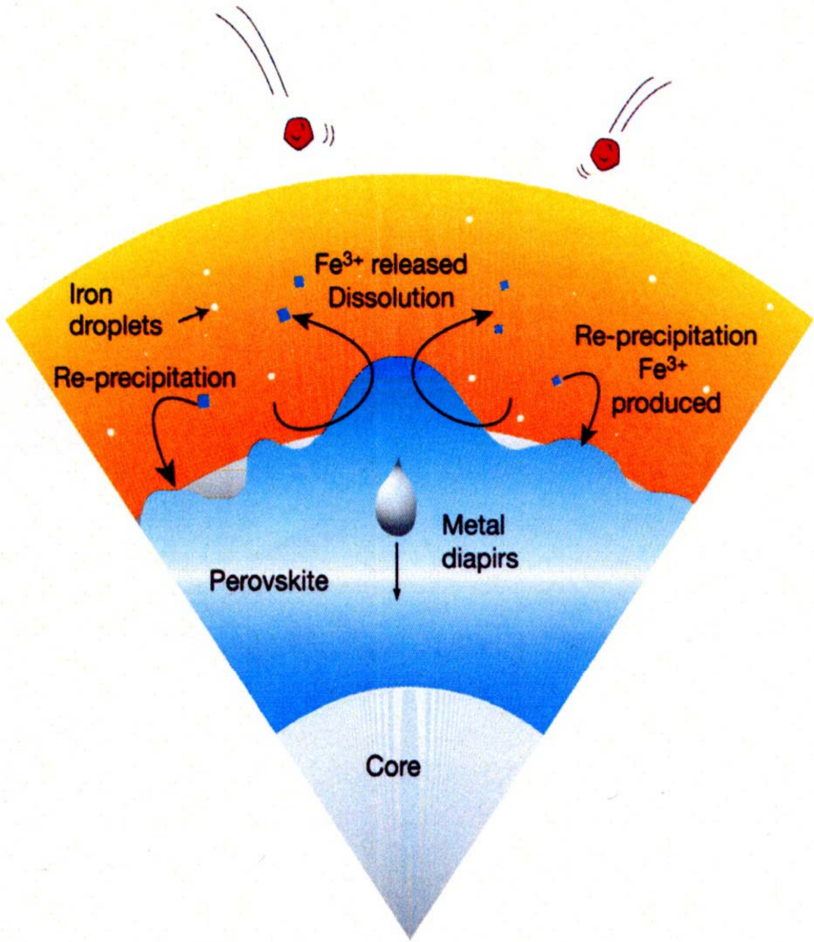


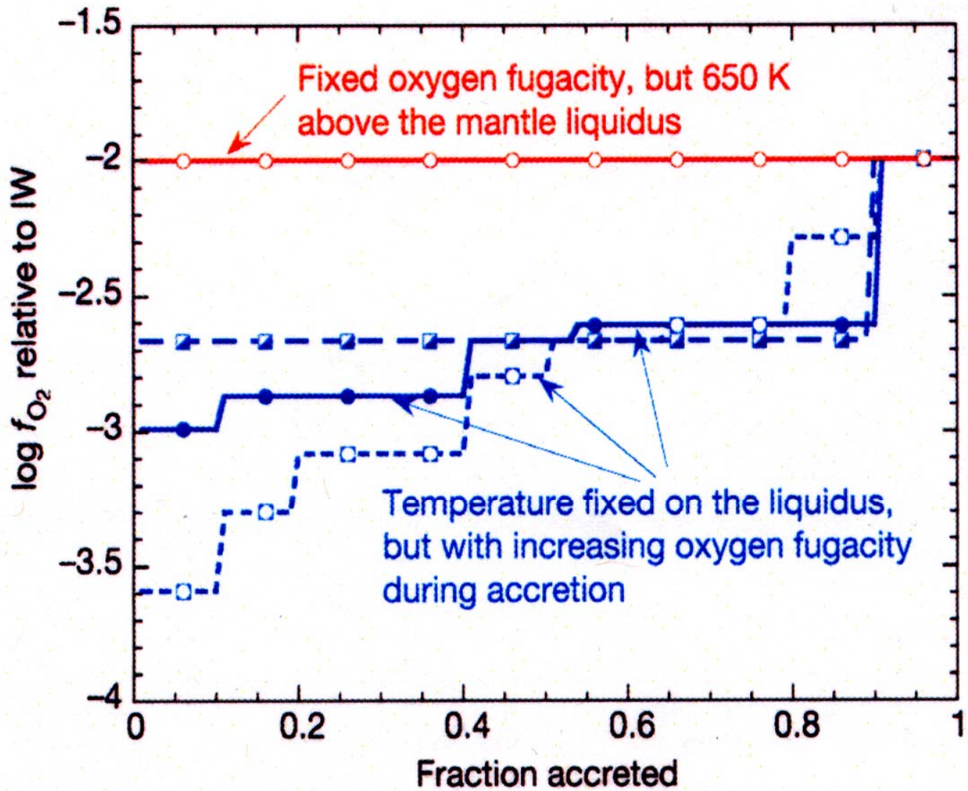

# Terrestrial Accretion under oxidising conditions

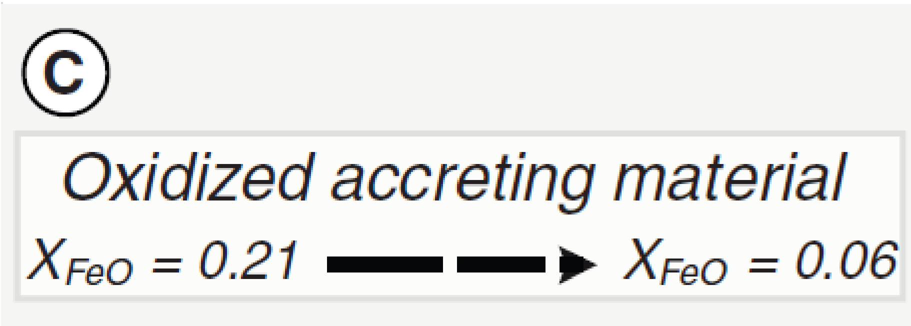


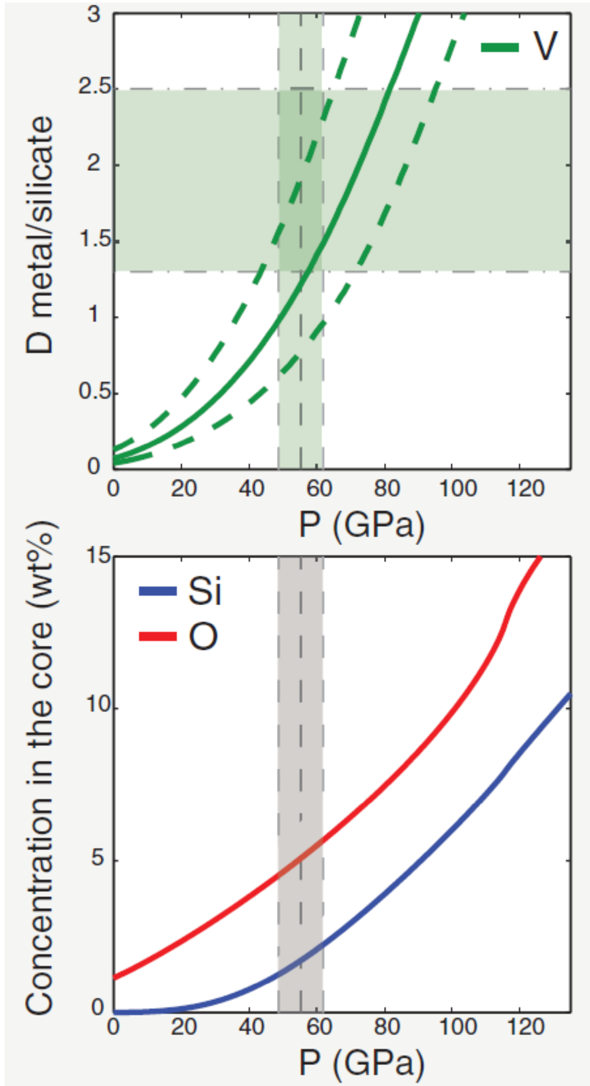


Siebert et al. (2013)

## "**N-body simulations**" dynamic system of particles, under gravity

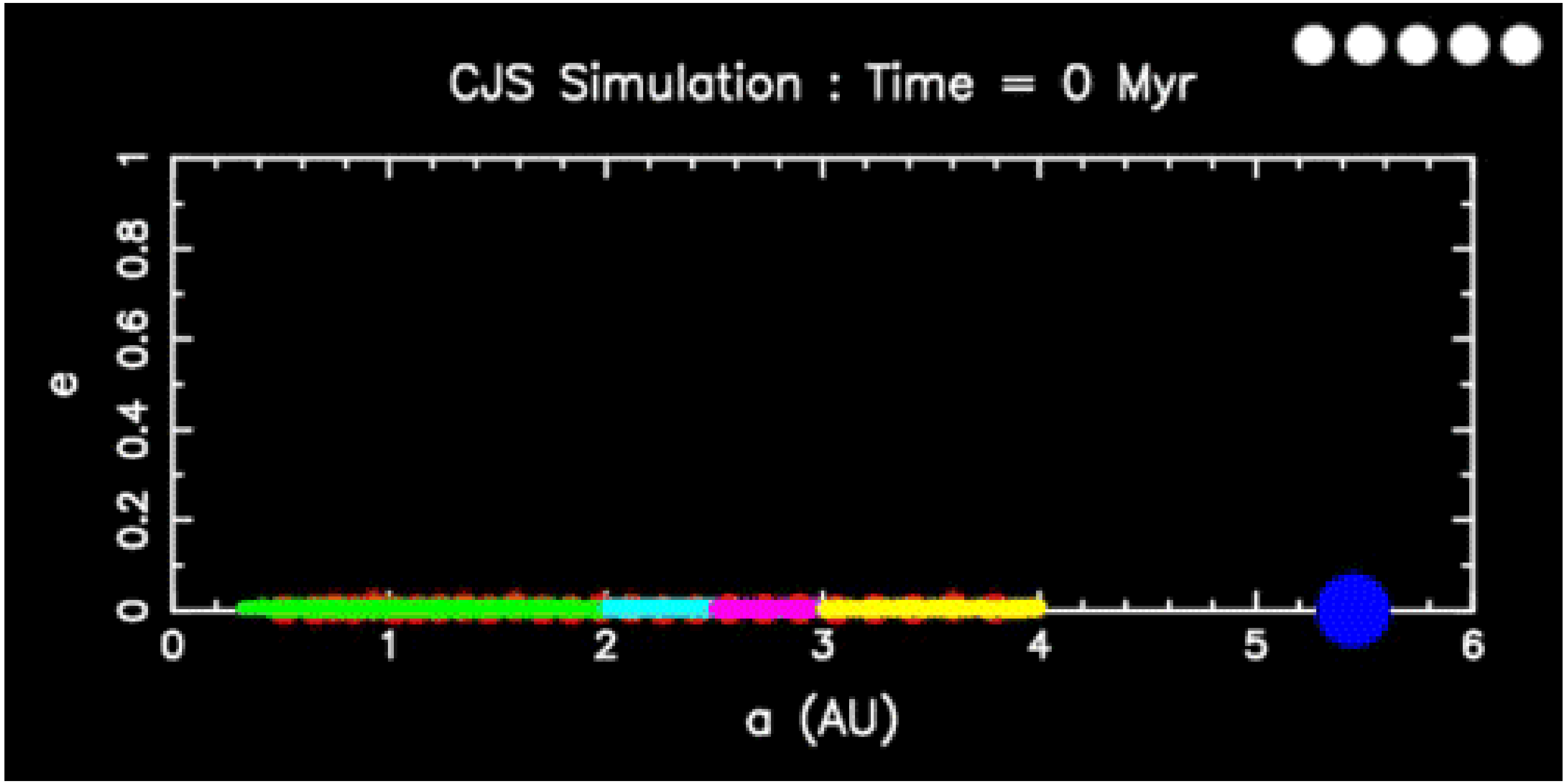


**<u>25-125 embryos</u>** (0.05-0.1$M_e$), **<u>1000-5500 planetesimals</u>** (0.0003-0.002 $M_e$)

(e.g. O'Brien et al., 2006; Walsh et al., 2011)

# Location and composition of final terrestrial planets

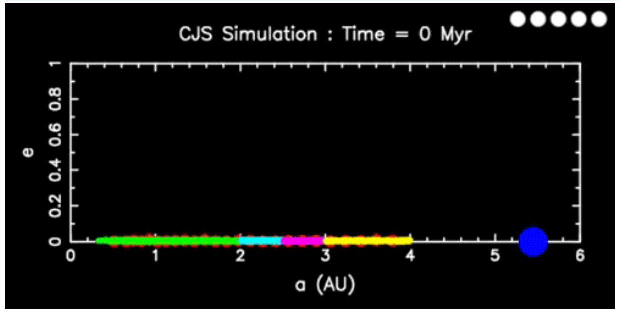


**Combine N-body simulations with**
**Core/mantle differentiation for each accretion event**

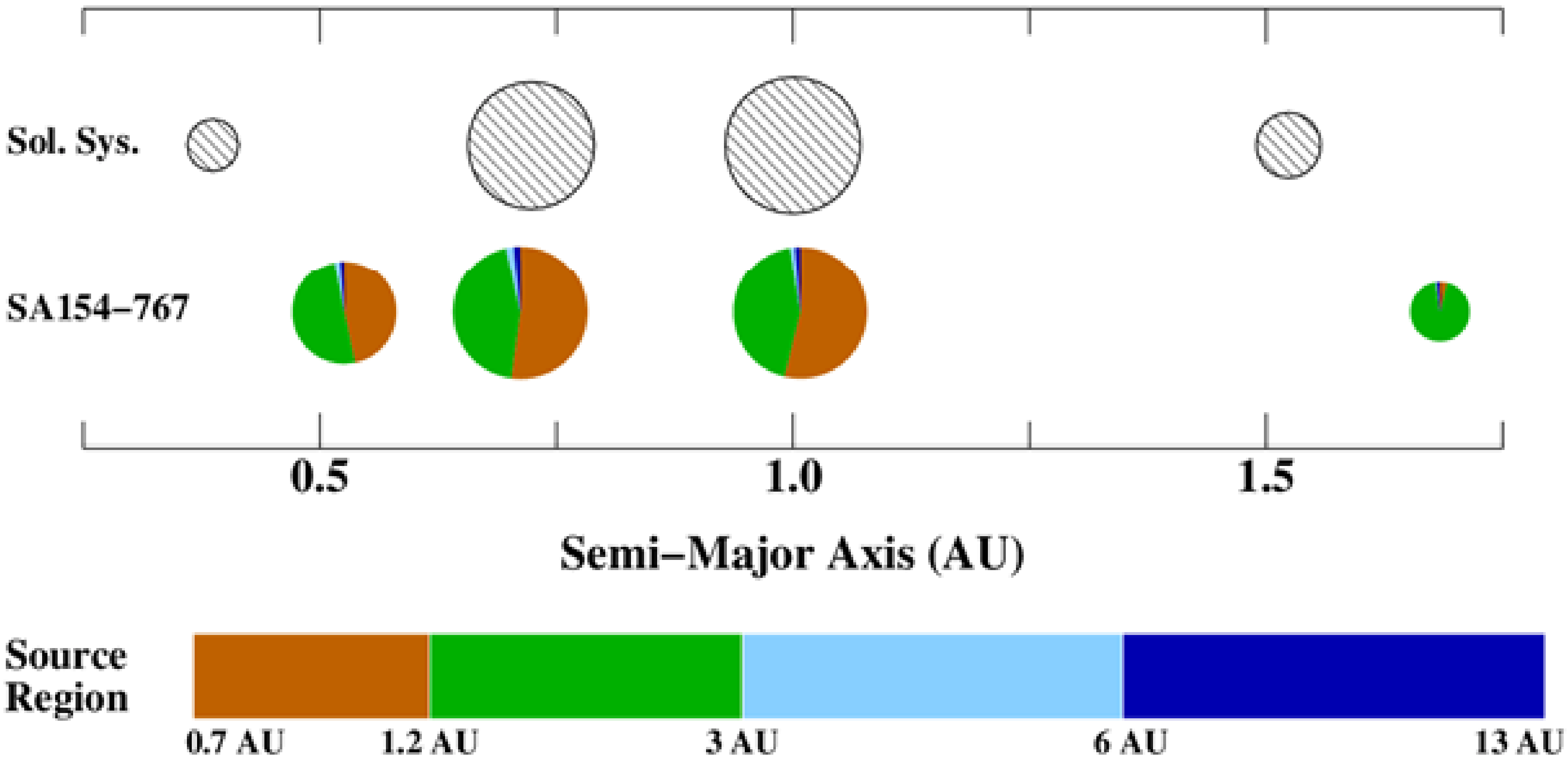

# Earth depleted in volatiles like all chondrites relative to CI

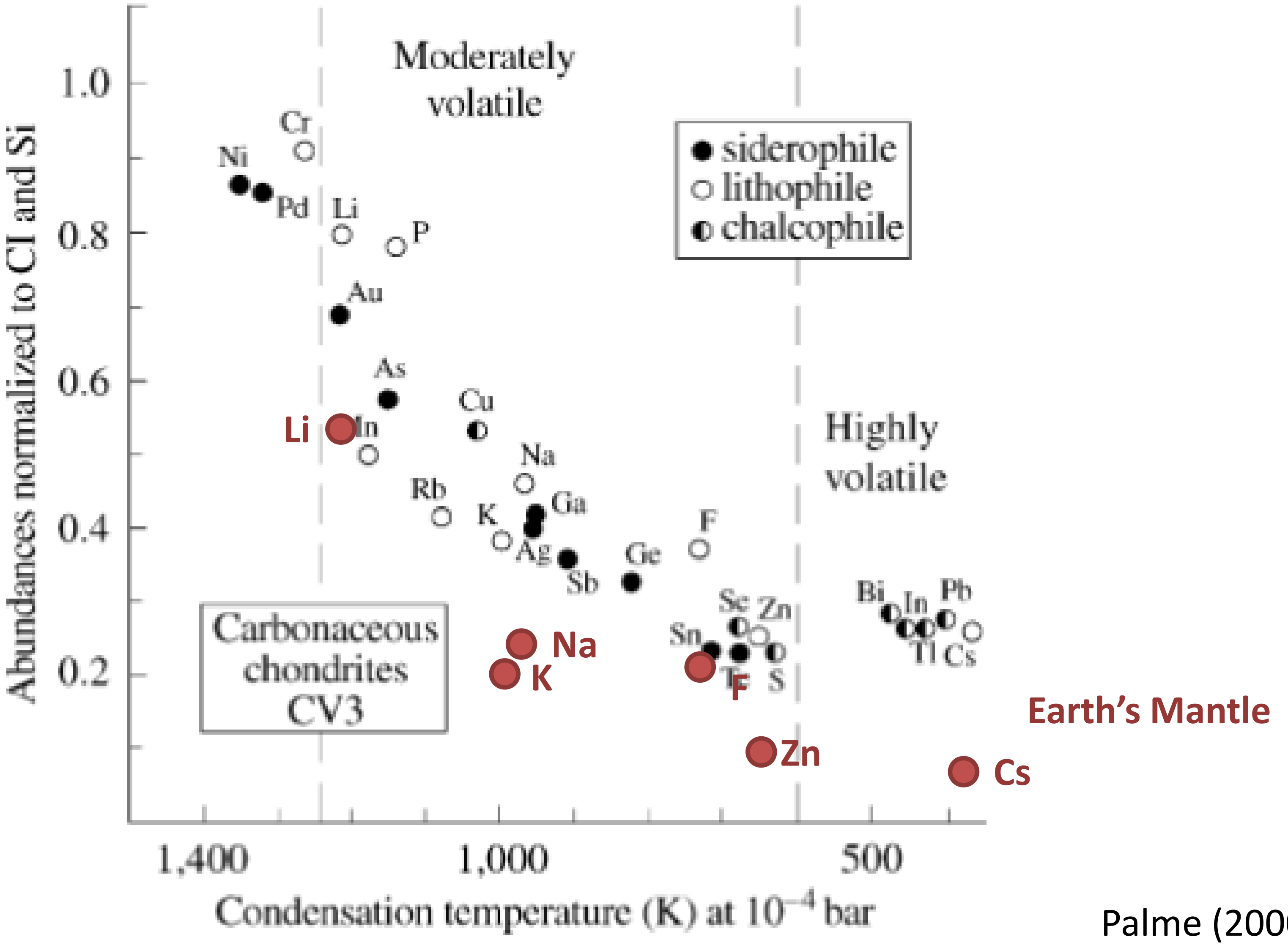


Palme (2000)

# Volatile depletion based on models for condensation

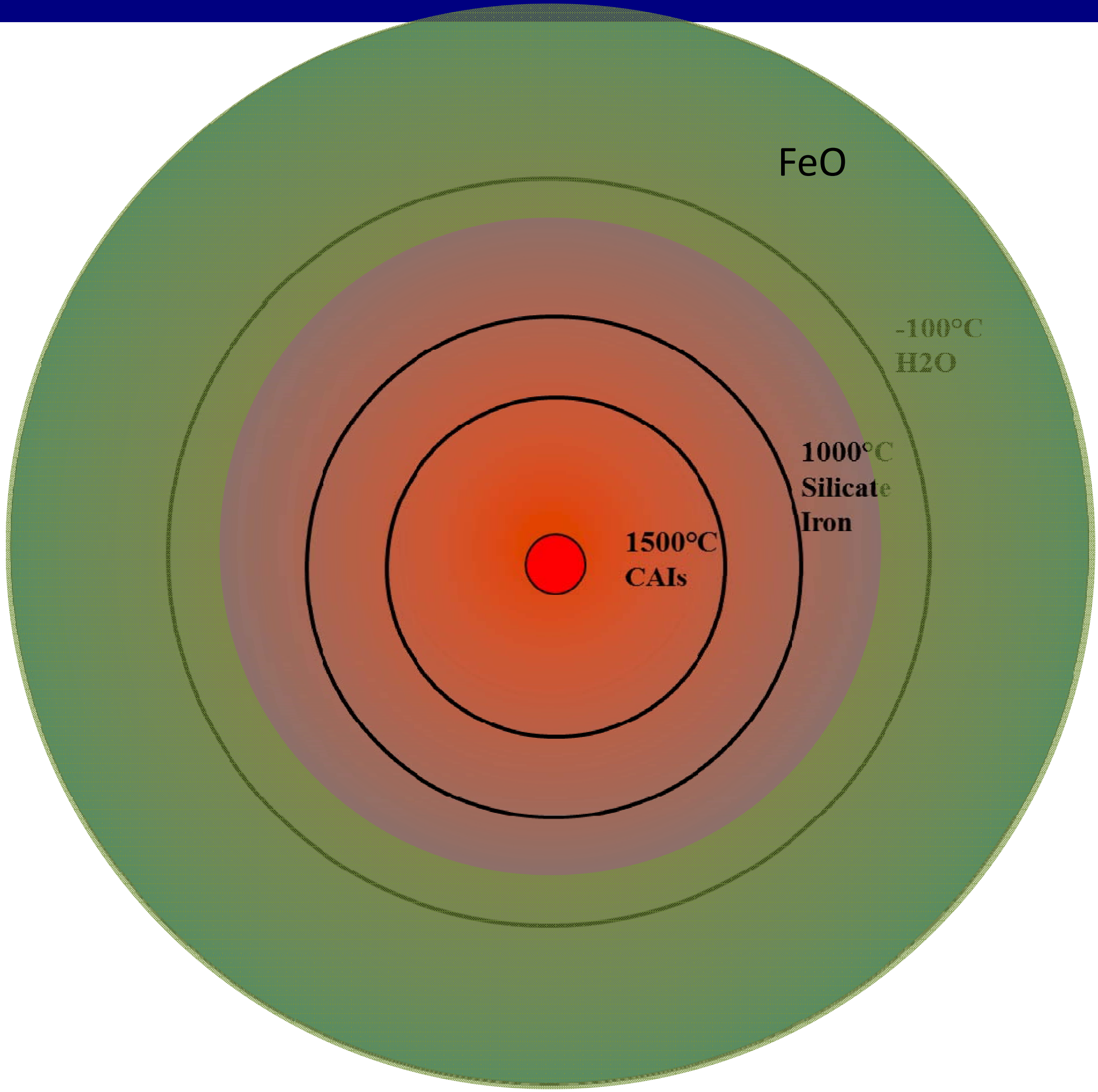


$H_2O + Fe \rightarrow FeO + H_2$

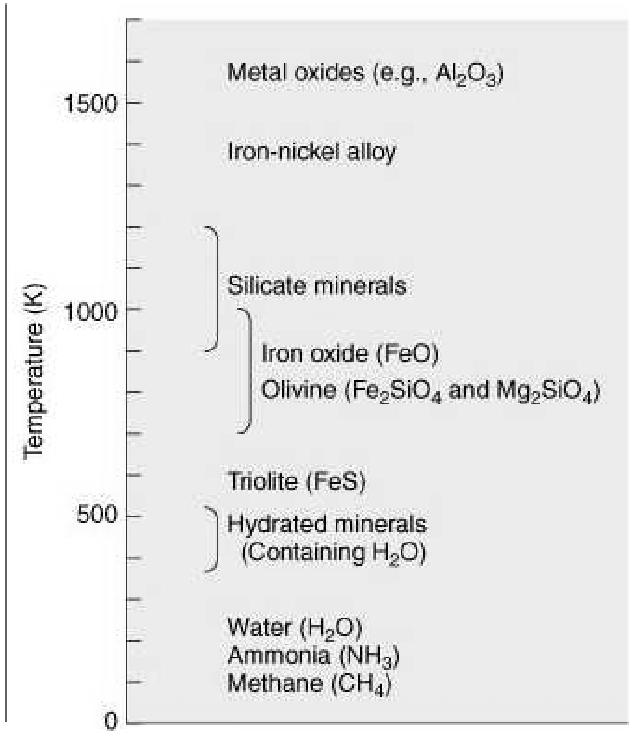

# Preferred composition-distance model

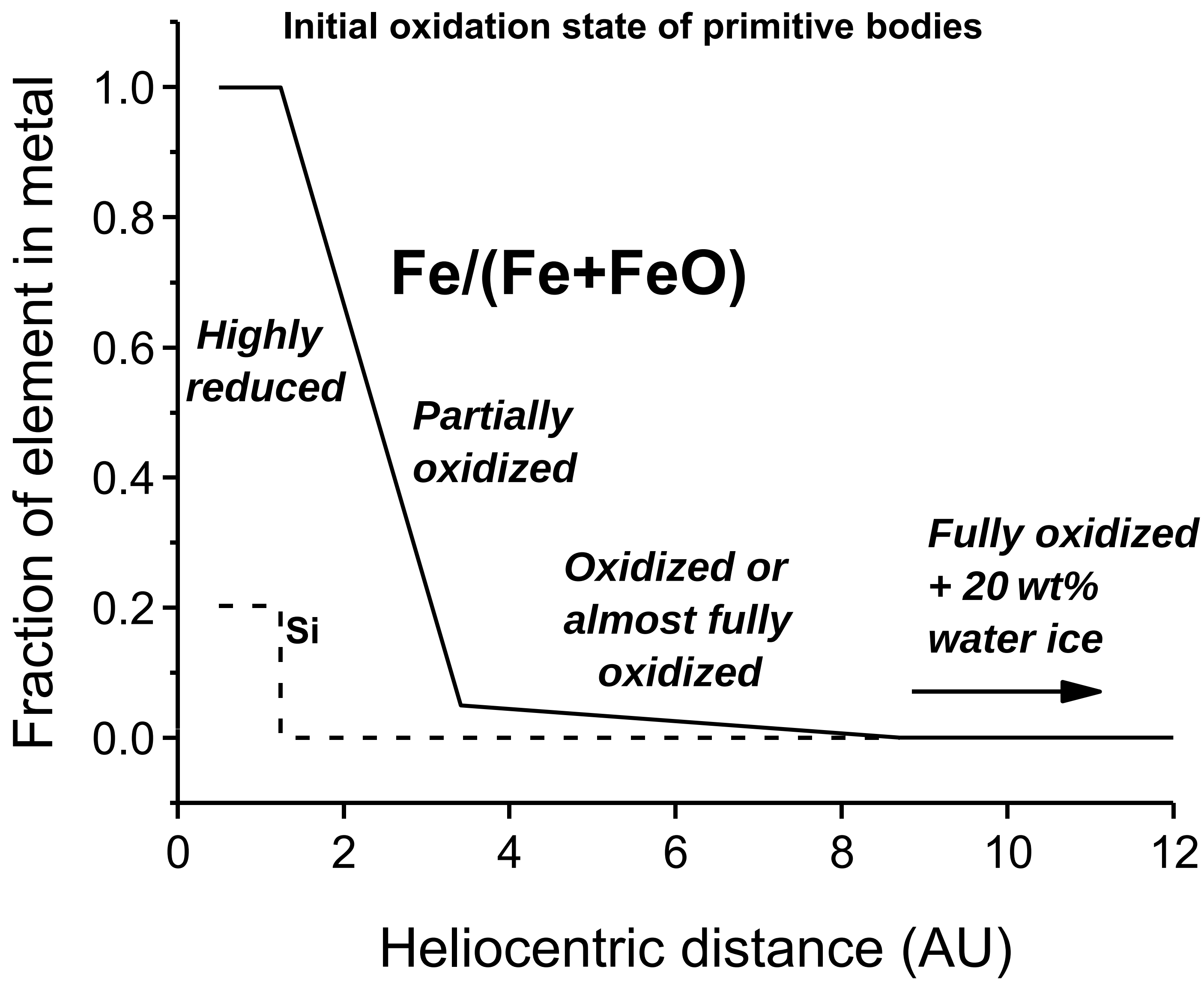


Rubie et al. 2014

# Mass balance approach to core formation modeling

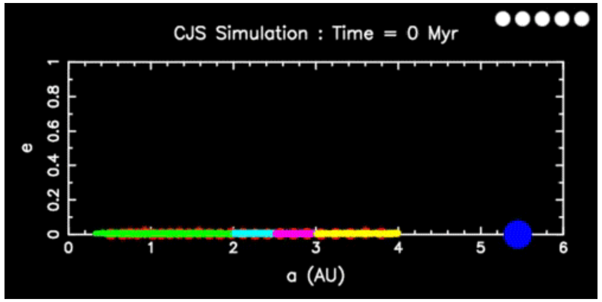


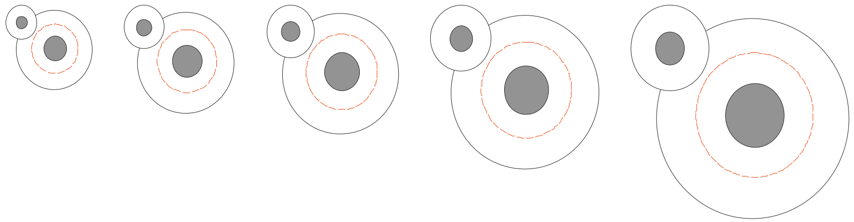

1) bulk composition of accreting material – solar system (CI) ratios of non-volatile elements but with oxygen contents varying over a radial gradient

2) Determine equilibrium compositions of co-existing silicate and metal liquids at high *P-T*:

$$[(FeO)_x\ (NiO)_y\ (SiO_2)_z\ (Mg_u\ Al_m\ Ca_n)O] + [Fe_a\ Ni_b\ O_c\ Si_d]$$

*silicate liquid* *metal liquid*

3) Maintain a mass balance- no assumed oxygen fugacity

# Proportion of a target's mantle/magma ocean that equilibrates with the impactor's core

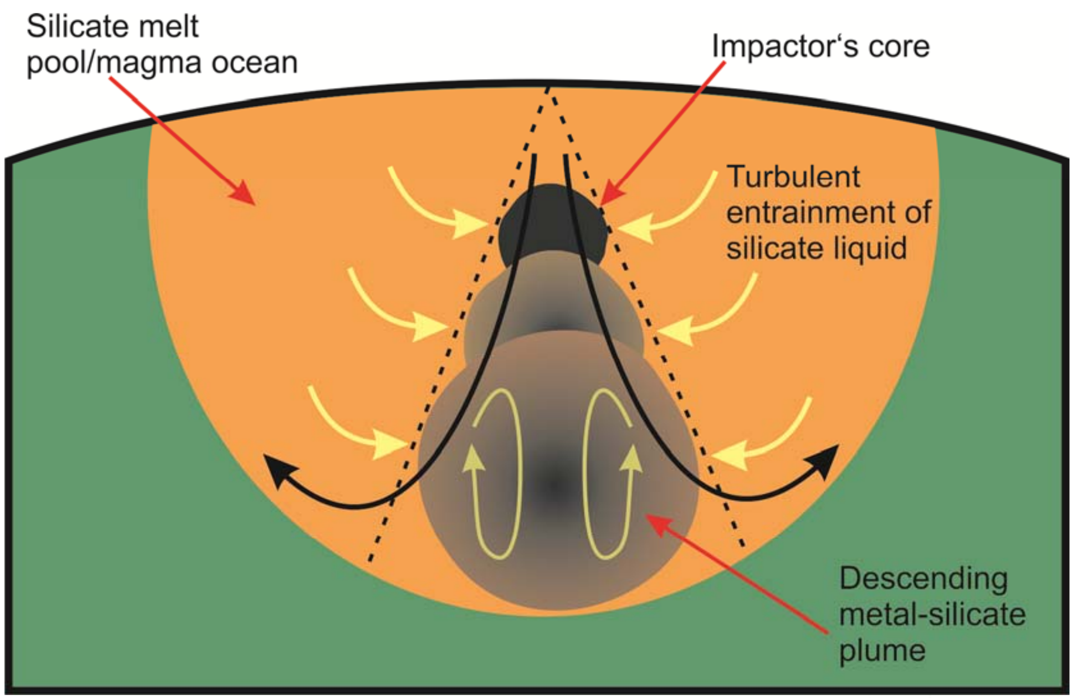


$$\phi = \left(\frac{r_0}{r}\right)^3 = \left(1 + \frac{\alpha z}{r_0}\right)^{-3}$$

where Φ is the volume fraction of metal in the metal-silicate mixture

Fraction of equilibrating mantle:

- 0.35-1.7% for planetesimal impacts
- 2-10% for embryo impacts

(Deguen et al., 2011, EPSL)

# Metal/Silciate partition coefficents at high P/T

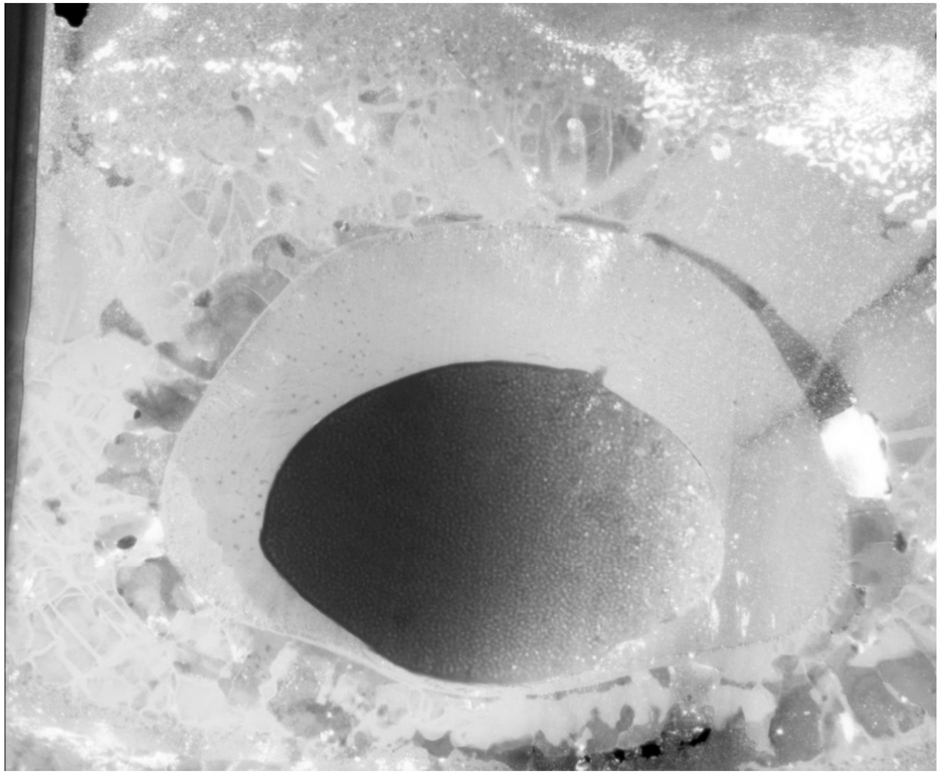

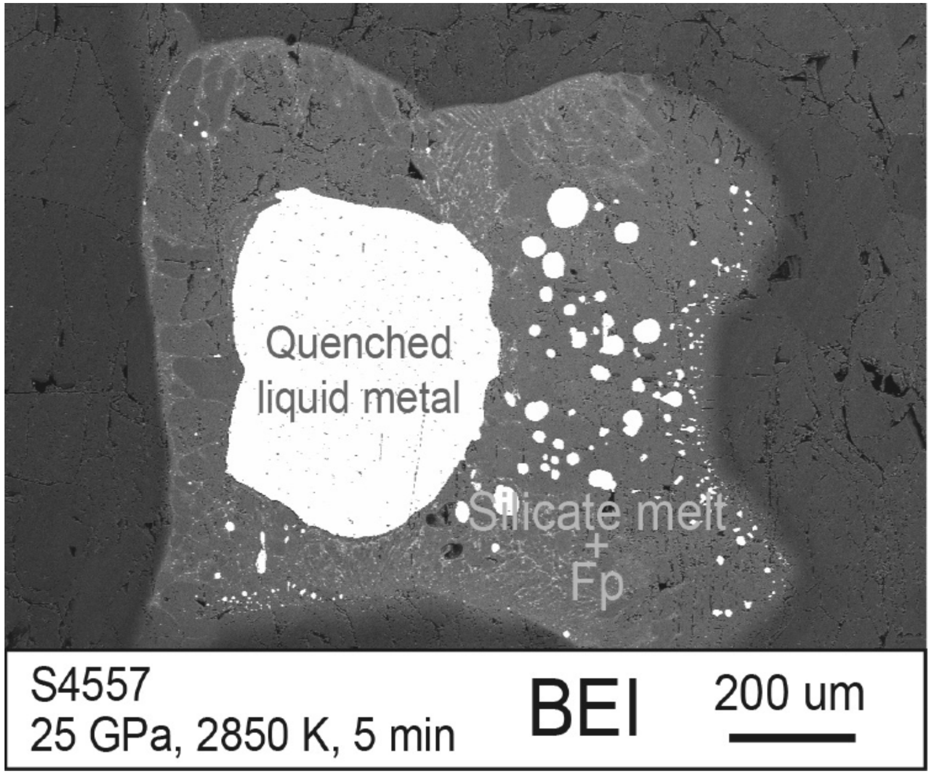


Laser heated diamond anvil cell

Up to 100 GPa

Multianvil

# Multistage Homogeneous Core formation

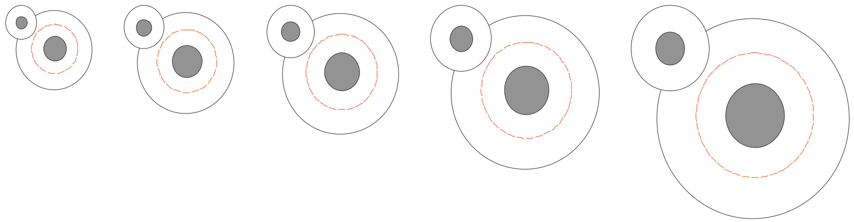

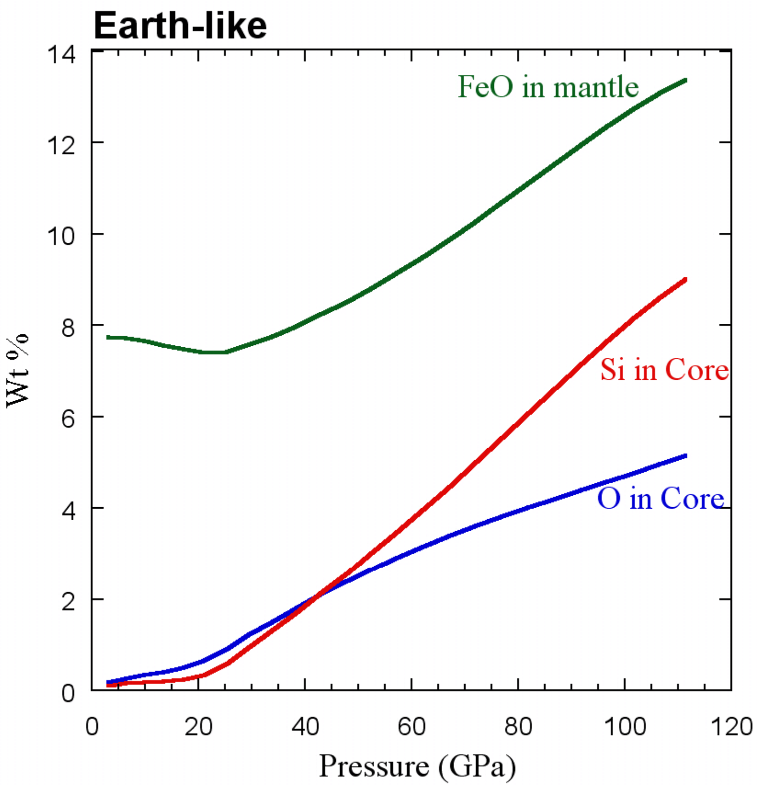


$$2Fe + SiO_2 = Si + 2FeO$$

Metal Silicate Metal Silicate

# Accretion history of Grand Tack simulation

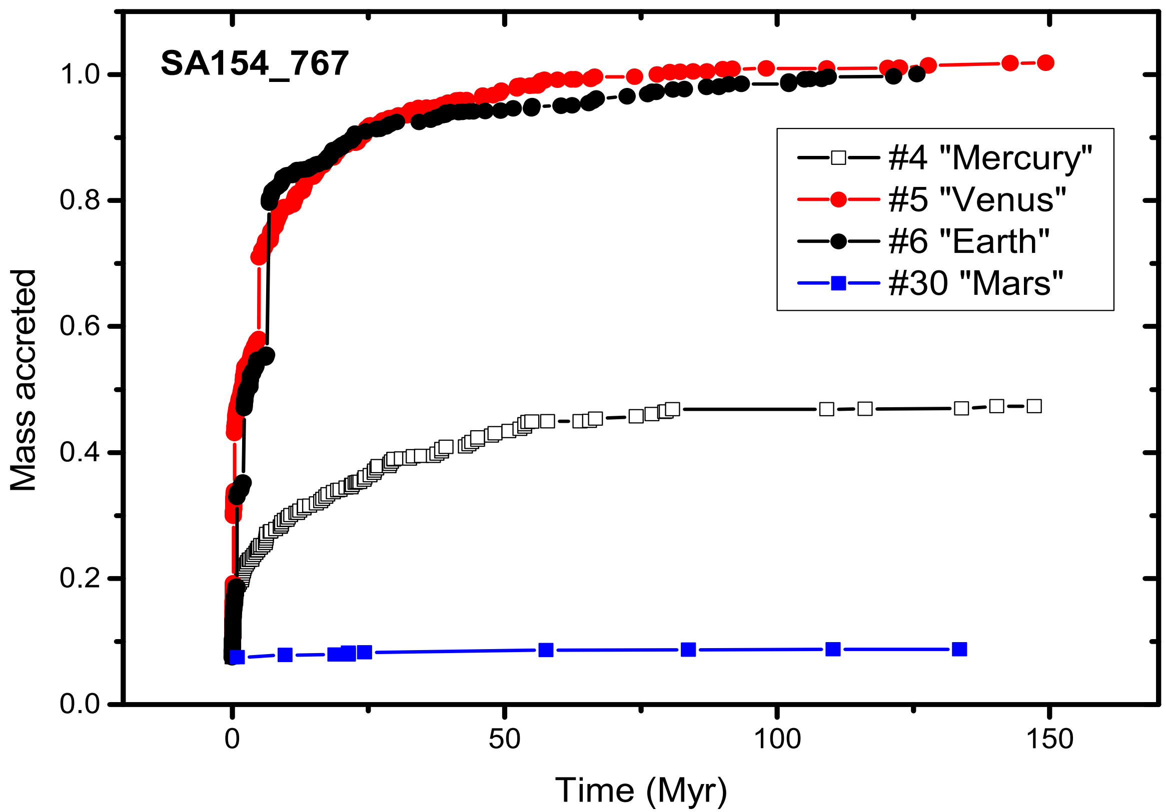


**Each accretion event (collision) results in an episode of core formation**

**Core formation and the evolving mantle and core chemistry are modelled in all the terrestrial planets simultaneously**

# Homogeneous accretion models

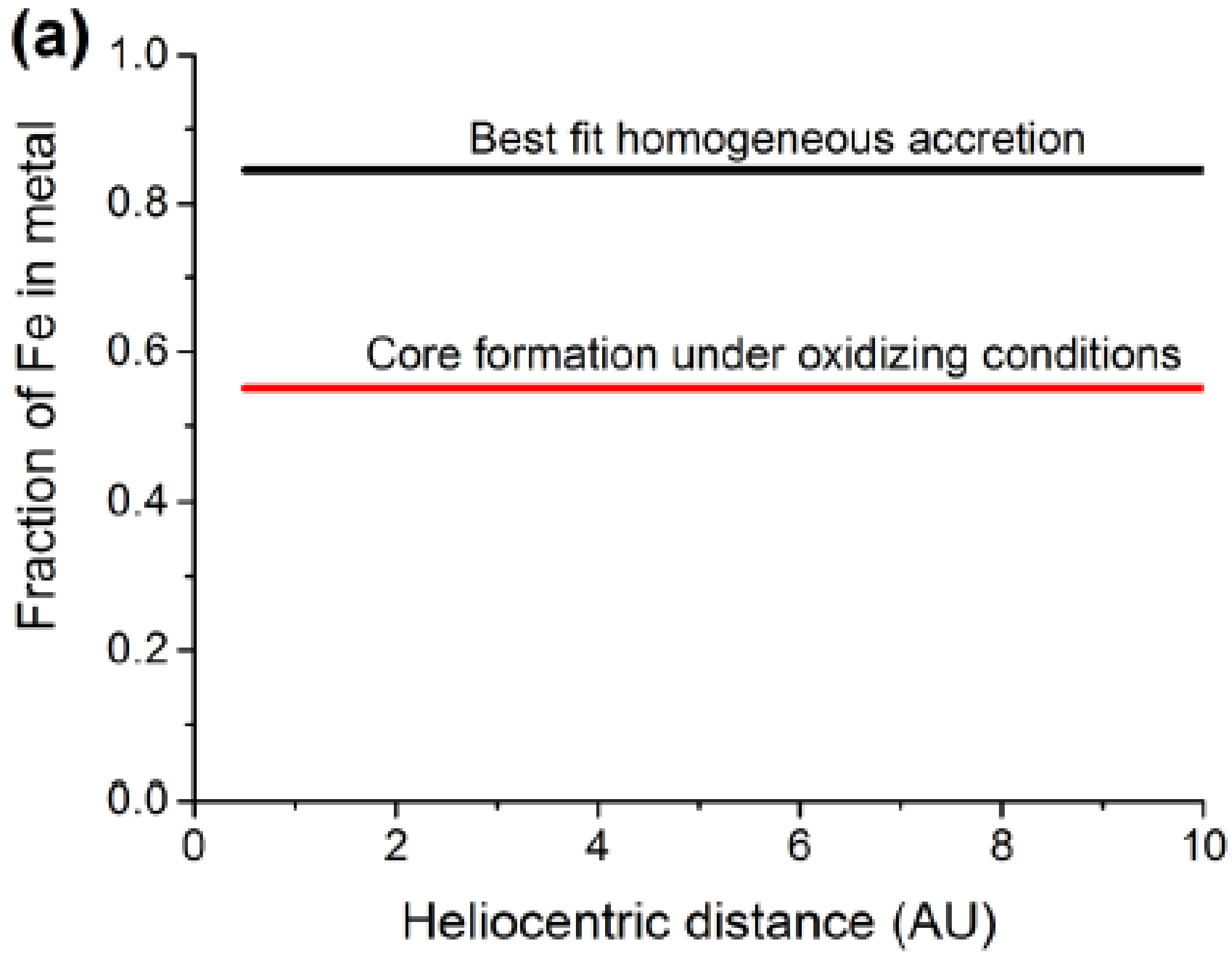

# Evolution of Earth's mantle composition based on two homogeneous accretion models

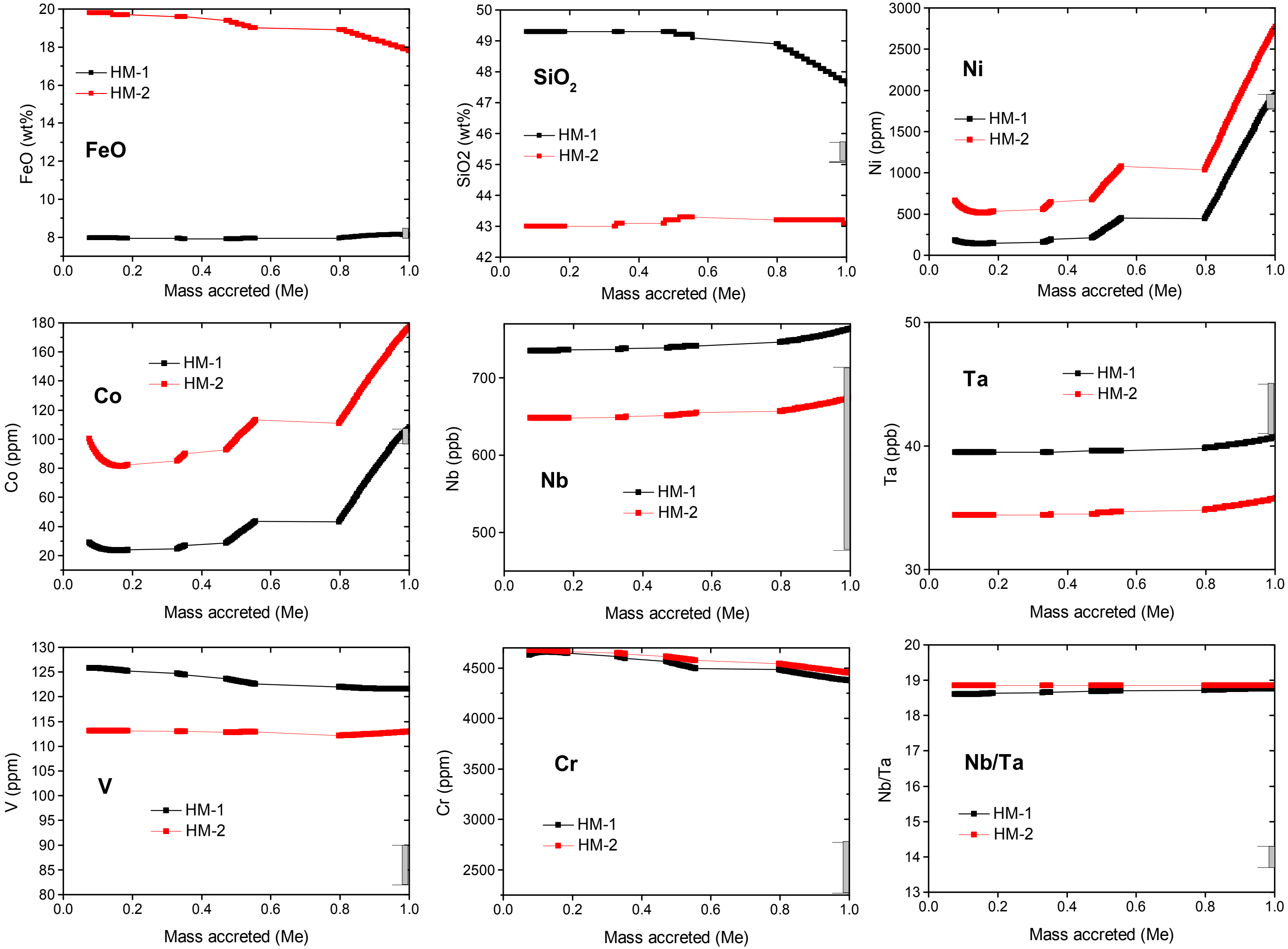

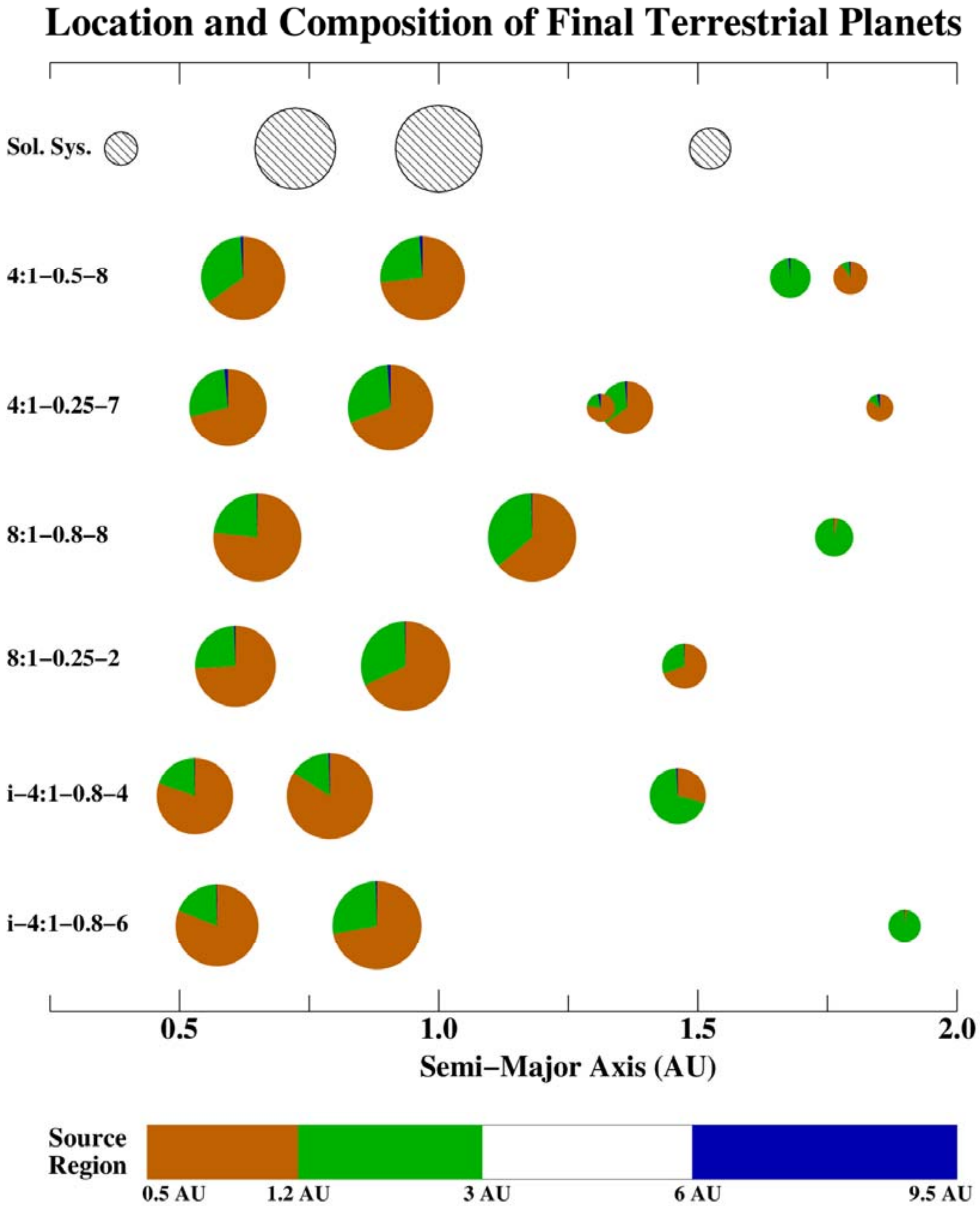
Location and Composition of Final Terrestrial Planets
Sol. Sys.
4:1–0.5–8
4:1–0.25–7
8:1–0.8–8
8:1–0.25–2
i–4:1–0.8–4
i–4:1–0.8–6
0.5
1.0
1.5
2.0
Semi–Major Axis (AU)
Source Region
0.5 AU
1.2 AU
3 AU
6 AU
9.5 AU

# $H_2O$ content of the mantle

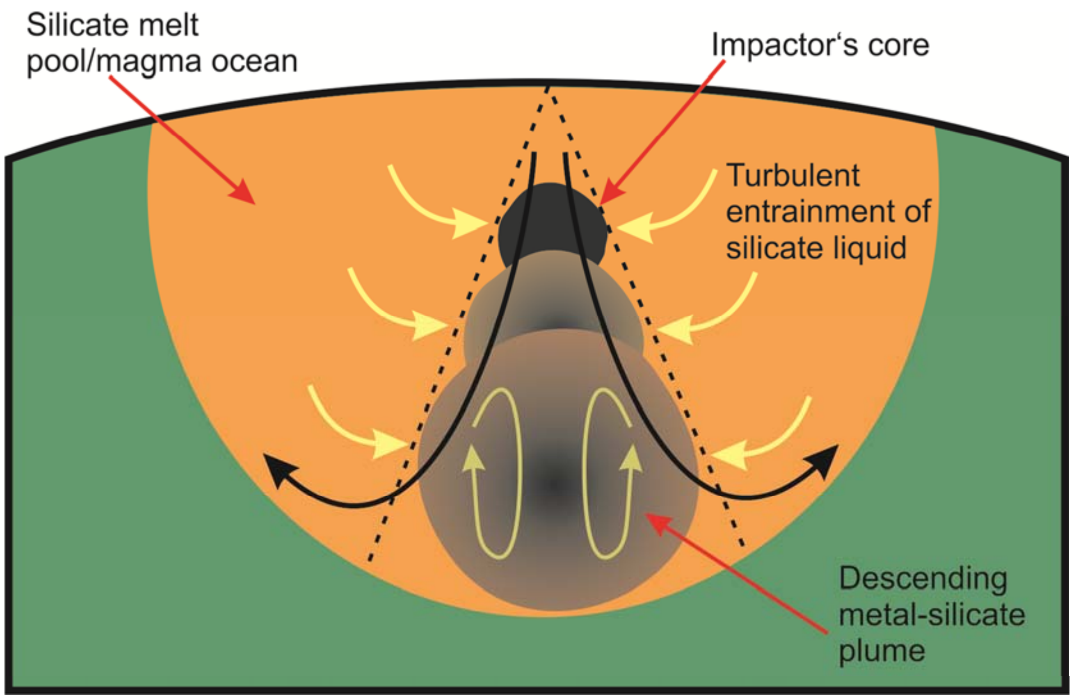


$H_2O + Fe \rightarrow FeO + H_2$

(Deguen et al., 2011, EPSL)

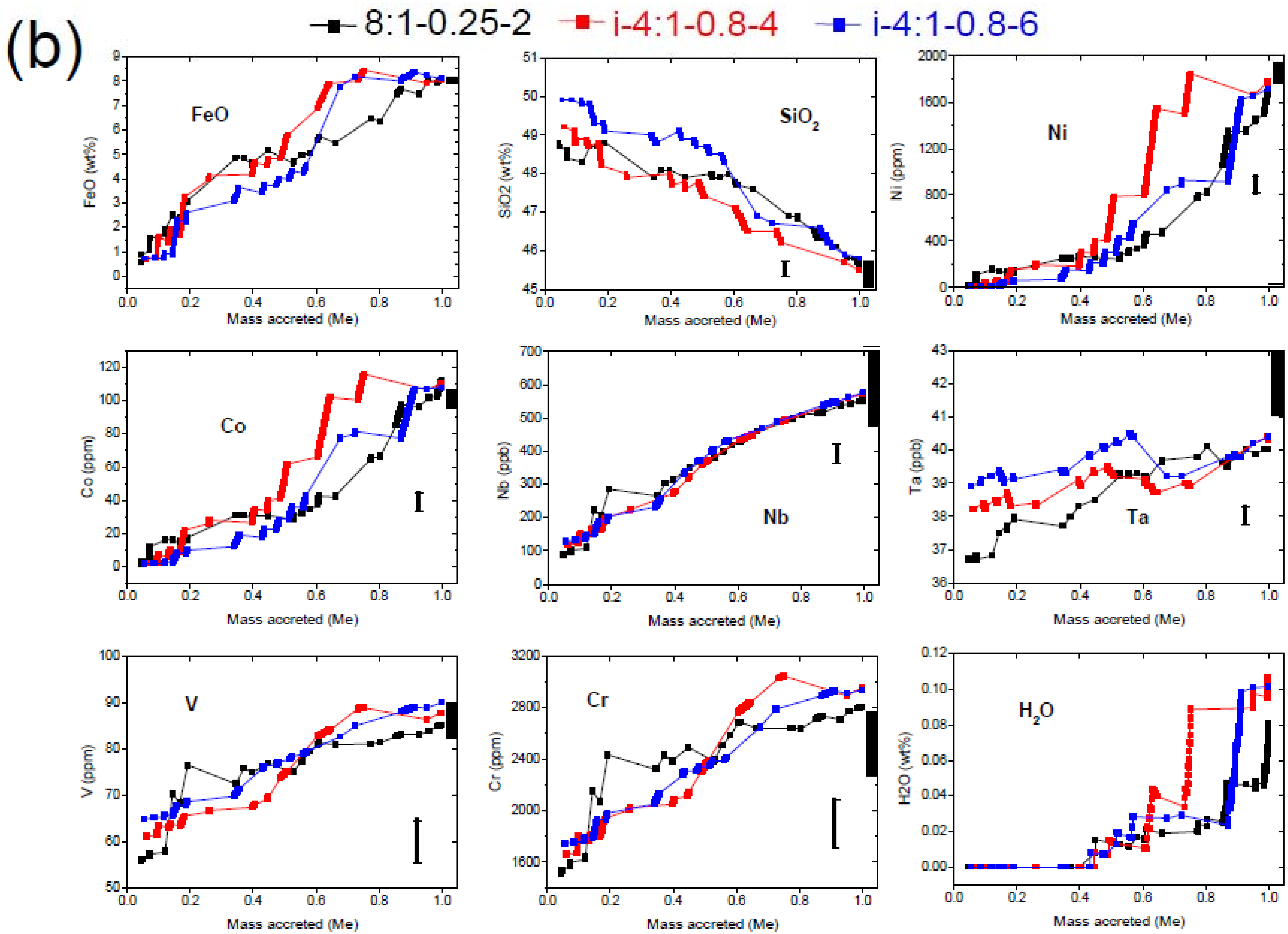
(b)
8:1-0.25-2
i-4:1-0.8-4
i-4:1-0.8-6
FeO
FeO (wt%)
SiO2
SiO2 (wt%)
Ni
Ni (ppm)
Co
Co (ppm)
Nb
Nb (ppb)
Ta
Ta (ppb)
V
V (ppm)
Cr
Cr (ppm)
H2O
H2O (wt%)
Mass accreted (Me)

# Composition of Venus

| **Simulation:** | **4:1-0.5-8** | **4:1-0.25-7** | **8:1-0.8-8** | **8:1-0.25-2** | **i-4:1-0.8-4** | **i-4:1-0.8-6** |
|---|---|---|---|---|---|---|
| **Heliocentric distance** | 0.623 AU | 0.594 AU | 0.650 AU | 0.608 AU | 0.530 AU | 0.572 AU |
| **Mass** | 0.979 Me | 0.745 Me | 0.987 Me | 0.766 Me | 0.701 Me | 0.808 Me |
| **Mantle compositions** | | | | | | |
| $SiO_2$ | 45.7 | 46.0 | 47.2 | 46.5 | 46.1 | 47.1 |
| FeO | 7.38 | 8.25 | 4.52 | 7.13 | 7.92 | 5.92 |
| $H_2O$ ppm | 824 | 1190 | 884 | 1515 | 580 | 773 |
| Mass % accreted from $H_2O$-bearing bodies | 0.27 % | 0.31 % | 0.29 % | 0.50 % | 0.20 % | 0.27 |
| **Core compositions and mass fractions** | | | | | | |
| O | 3.14 | 2.08 | 2.66 | 0.73 | 1.47 | 1.27 |
| Si | 9.11 | 7.29 | 8.26 | 7.57 | 7.61 | 7.45 |

# Composition of Martian Mantle

| **Simulation:** | | **4:1-0.5-8 "Mars 2"** | **4:1-0.25-7 "Mars-1"** | **4:1-0.25-7 "Mars-3"** | **8:1-0.8-8** | **i-4:1-0.8-6** |
|---|---|---|---|---|---|---|
| **HD of origin:**<br>**Final HD:**<br>**Mass:** | **1.52 AU**<br>**0.107 $M_e$** | **1.14 AU**<br>**1.79 AU**<br>**0.064 $M_e$** | **1.13 AU**<br>**1.31 AU**<br>**0.035 $M_e$** | **1.16 AU**<br>**1.85 AU**<br>**0.032 $M_e$** | **1.53 AU**<br>**1.76 AU**<br>**0.081 $M_e$** | **1.58 AU**<br>**1.90 AU**<br>**0.064 $M_e$** |
| **Martian mantle compositions** | | | | | | |
| | **Taylor (2013)** | | | | | |
| $SiO_2$ | 43.7 (1.0) | 50.5 | 47.3 | 49.5 | 47.2 | 42.3 |
| FeO | 18.1 (1.0) | 4.94 | 6.71 | 6.80 | 11.8 | 20.2 |
| Ni ppm | 330 (109) | 102 | 170 | 168 | 331 | 568 |
| Co ppm | 71 (25) | 17.3 | 29.4 | 28.5 | 51.2 | 92 |
| Nb ppb | 501 (7) | 621 | 258 | 569 | 696 | 644 |
| Ta ppb | 27.2 (1) | 40 | 37 | 39 | 38 | 34 |
| Nb/Ta | 19.9 (0.06)* | 15.4 | 7.0 | 14.5 | 18.4 | 18.8 |
| V ppm | 60-105 (R&C) | 112 | 75 | 109 | 121 | 113 |
| Cr ppm | 4990 (420) | 3534 | 2437 | 3415 | 4651 | 4653 |
| $H_2O$ ppm | | 1786 | 2225 | 4769 | 399 | 0 |
| Mass % accreted from $H_2O$-bearing bodies | | 0.57% | 0.68% | 1.51% | 0.13% | 0.0% |

# Evolution of a layered structure – results of 100 N-body simulations

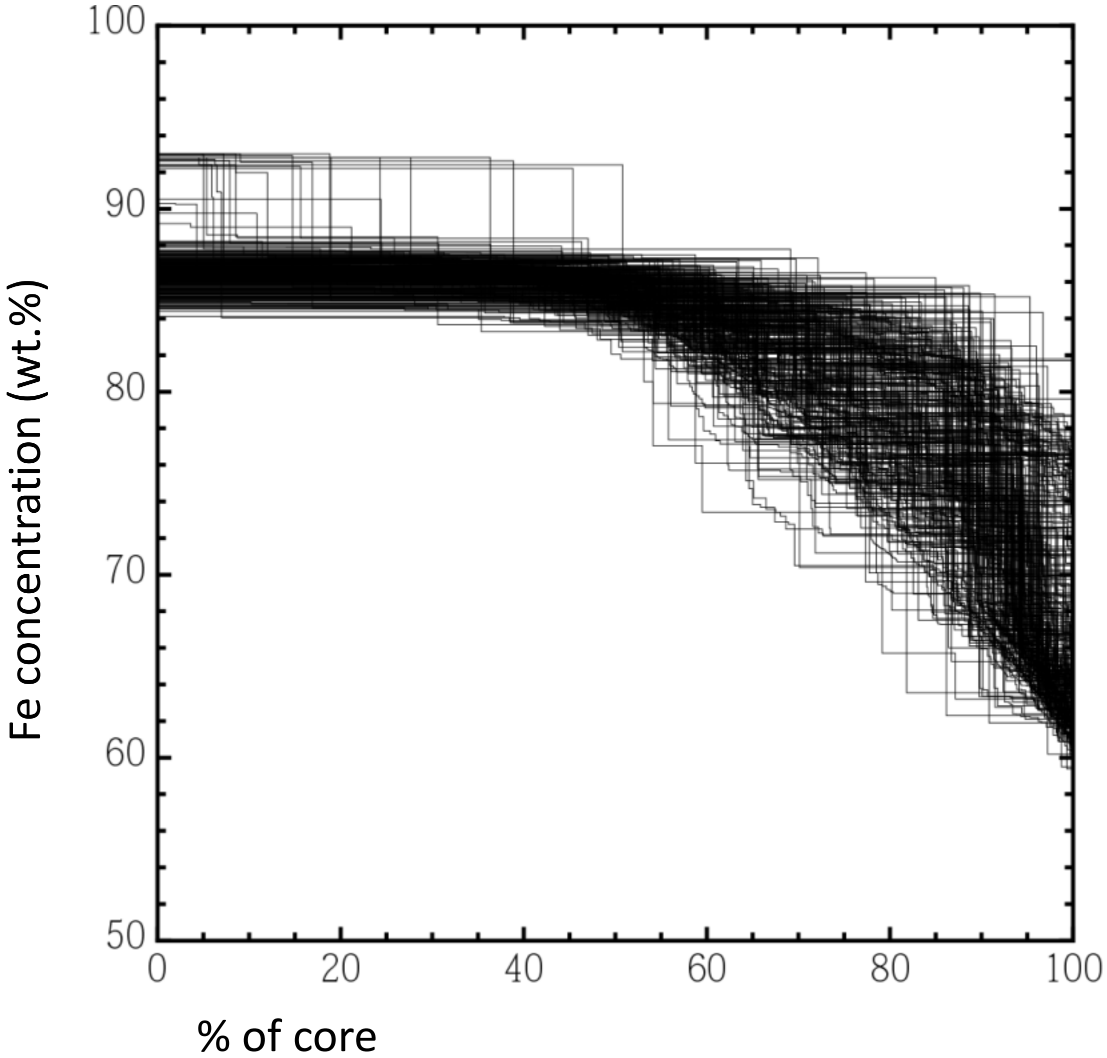

# Summary

- Combining N-body accretion and core formation models enables the evolution of core and mantle compositions to be modelled
- $H_2O$ could have been accreted relatively early
- Using this approach, the cores of Earth and Venus are predicted to contain 7 wt% silicon and 3 wt% oxygen
- Partitioning of oxygen and silicon into liquid Fe is enhanced by high temperature and batches of core-forming metal contain high concentrations of these elements during late accretion
- Development of a density stratification is inevitable in Earth-mass planets but may be destroyed by a giant impact
- The lack of a magnetic field on Venus may indicate a stratified core which has survived due to an absence of late giant impacts

# Evolution of the concentration of light elements in Earth’s core

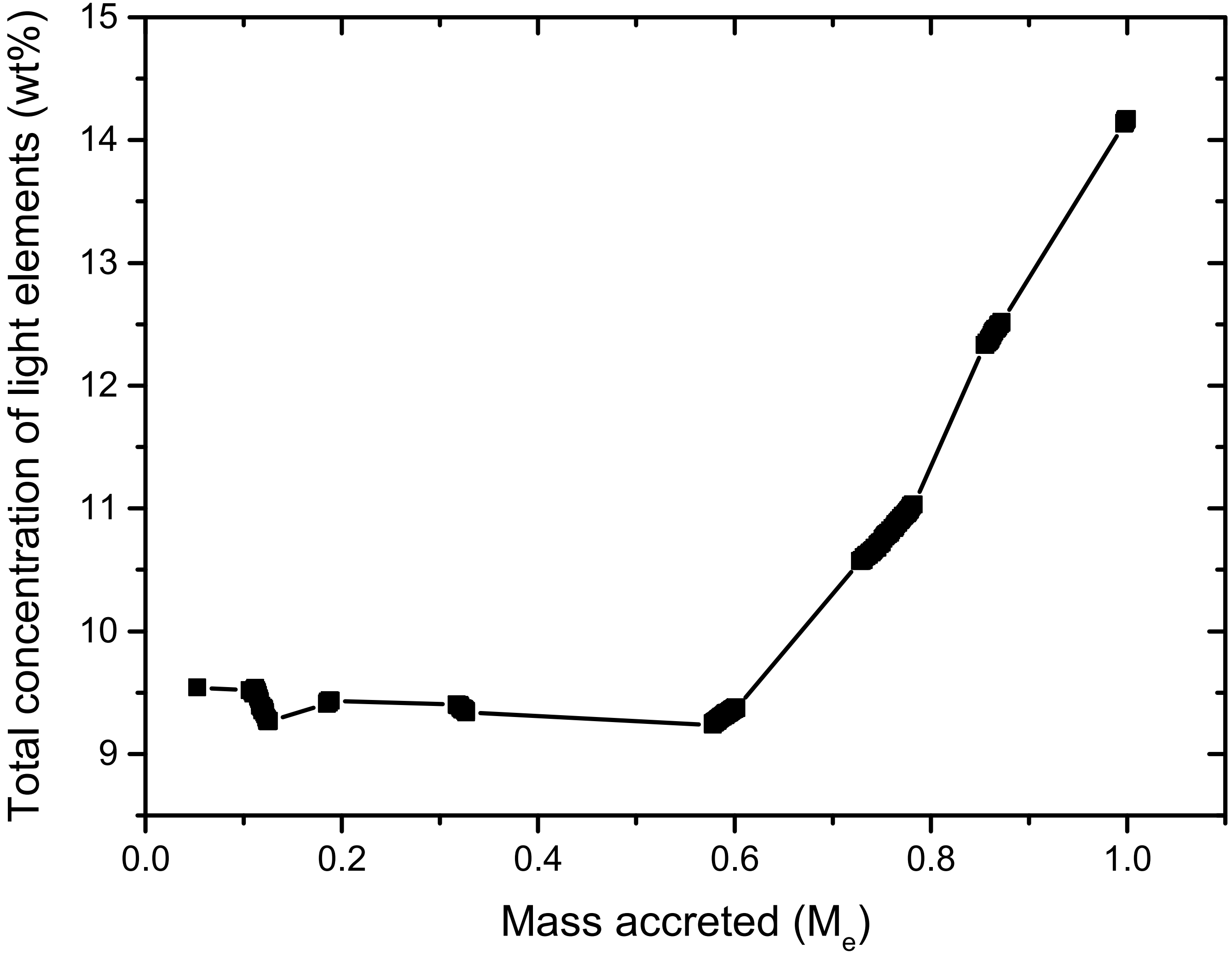

| **Simulation:** | | **4:1-0.5-8** | **4:1-0.25-7** | **8:1-0.8-8** | **8:1-0.25-2** | **i-4:1-0.8-4** | **i-4:1-0.8-6** |
|---|---|---|---|---|---|---|---|
| **Heliocentric distance** | | 0.969 AU | 0.907 AU | 1.18 AU | 0.936 AU | 0.79 AU | 0.88 AU |
| **Mantle compositions** | | | | | | | |
| | **Earth PM** | | | | | | |
| $SiO_2$ | **45.40 (0.30)** | 45.4 (0.1) | 45.3 (0.1) | 45.5 (0.1) | 45.6 (0.1) | 45.5 (0.1) | 45.8 (0.1) |
| FeO | **8.10 (0.05)** | 8.09 (0.01) | 8.09 (0.01) | 8.10 (0.01) | 8.12 (0.01) | 8.08 (0.01) | 8.10 (0.01) |
| Ni ppm | **1860 (93)** | 1820 (321) | 1810 (404) | 1750 (265) | 1705 (222) | 1770 (295) | 1714 (294) |
| Co ppm | **102 (5)** | 108 (19) | 106 (23) | 115 (15) | 112 (14) | 110 (18) | 108 (19) |
| Nb ppb | **595 (119)** | 557 (35) | 578 (38) | 567 (42) | 553 (31) | 572 (28) | 576 (25) |
| Ta ppb | **43 (2)** | 40 (1) | 41 (1) | 41 (1) | 40 (1) | 40 (1) | 40 (1) |
| Nb/Ta | **14.0 (0.3)*** | 13.8 | 14.2 | 13.95 | 13.85 | 14.19 | 14.25 |
| V ppm | **86 (5)** | 89 (27) | 87 (29) | 84 (30) | 85 (28) | 88 (26) | 90 (28) |
| Cr ppm | **2520 (252)** | 2980 (426) | 2900 (415) | 2730 (452) | 2805 (433) | 2958 (424) | 2940 (449) |
| $H_2O$ ppm | **1160 (232)** | 1010 | 1000 | 793 | 806 | 1066 | 1013 |
| Mass % accreted from $H_2O$-bearing bodies | | 0.38 % | 0.34 % | 0.26 % | 0.27 % | 0.37 % | 0.36 % |
| **Core compositions and mass fractions** | | | | | | | |
| Fe | | 81.7 | 81.3 | 82.4 | 82.9 | 81.6 | 82.3 |
| Ni | | 5.14 | 4.99 | 5.23 | 5.28 | 5.16 | 5.23 |
| Co | | 0.24 | 0.23 | 0.24 | 0.24 | 0.24 | 0.24 |
| O | | 3.59 | 3.71 | 2.89 | 2.58 | 3.85 | 3.81 |
| Si | | 8.65 | 9.03 | 8.51 | 8.23 | 8.40 | 7.73 |
| Nb ppb | | 557 | 532 | 533 | 562 | 514 | 500 |
| Ta ppb | | 5.7 | 5.1 | 5.0 | 6.2 | 5.5 | 4.6 |
| V ppm | | 118 | 127 | 128 | 125 | 118 | 113 |
| Cr wt% | | 0.70 | 0.74 | 0.75 | 0.74 | 0.69 | 0.70 |
| H ppm | | 58 | 28 | 14 | 22 | 34 | 40 |
| Core mass fraction | **0.32** | 0.312 | 0.306 | 0.313 | 0.311 | 0.314 | 0.311 |

# Metal/Silciate partition coefficents at high P/T

$$K_{D(P,T)} = \frac{\left[X_{Si}^{Met}\right]\left[X_{FeO}^{Silciate}\right]^2}{\left[X_{Fe}^{Met}\right]^2\left[X_{SiO_2}^{Silicate}\right]}$$

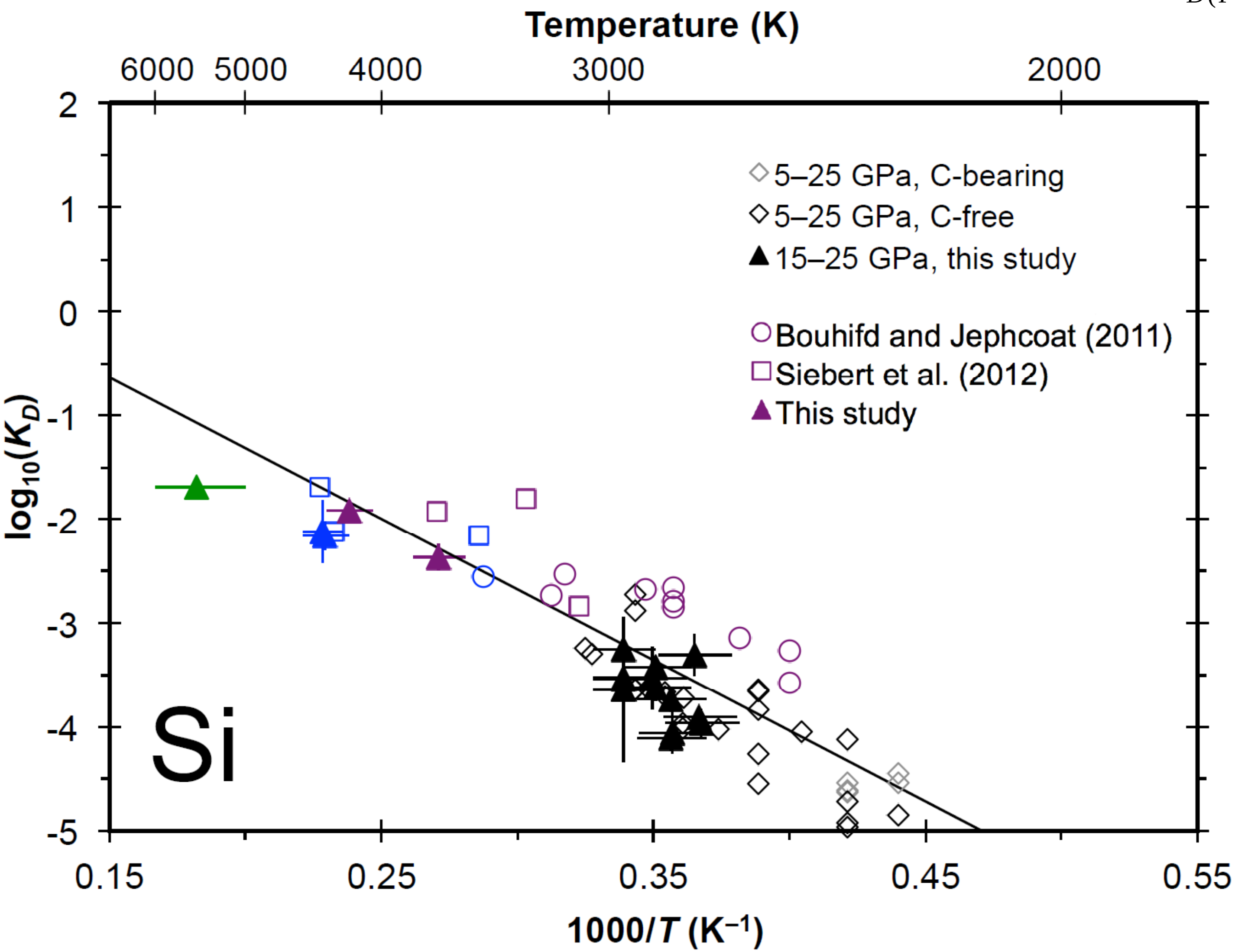

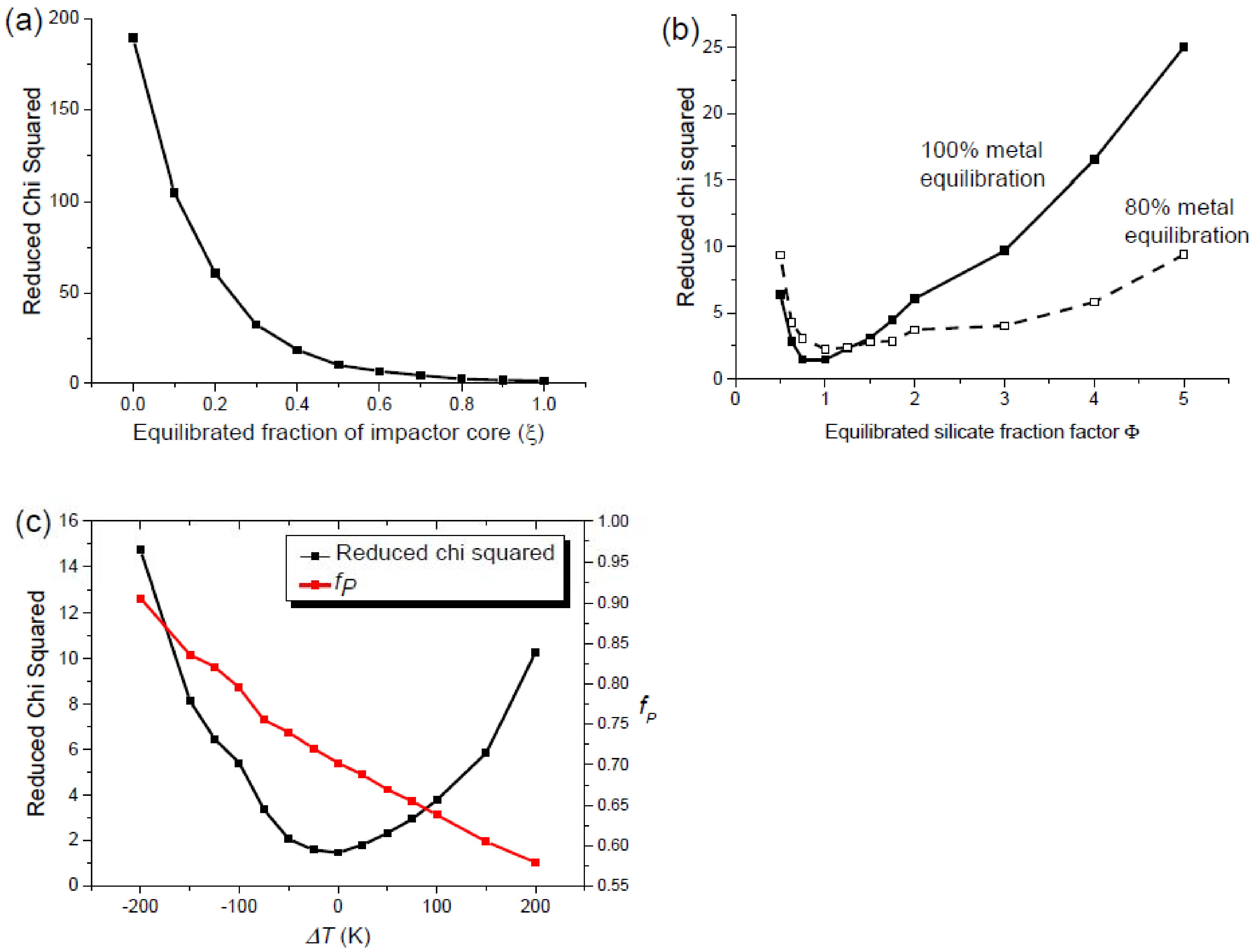
(a)
Reduced Chi Squared
Equilibrated fraction of impactor core (ξ)
(b)
Reduced chi squared
100% metal equilibration
80% metal equilibration
Equilibrated silicate fraction factor Φ
(c)
Reduced Chi Squared
Reduced chi squared
$f_P$
ΔT (K)

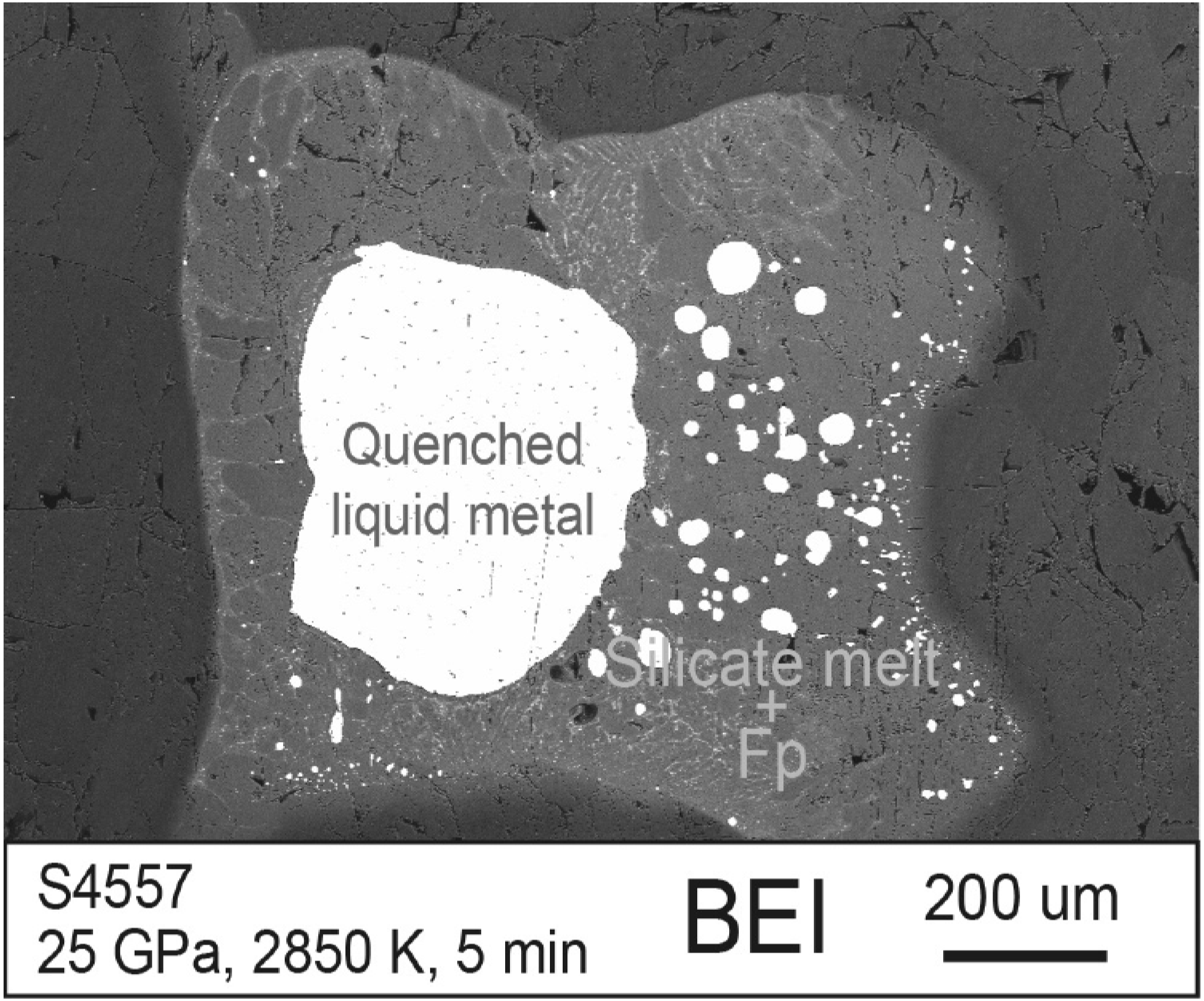
Quenched
liquid metal
Silicate melt
+
Fp
S4557
25 GPa, 2850 K, 5 min
BEI
200 um

# Evolution of Earth's mantle composition based on preferred composition-distance model

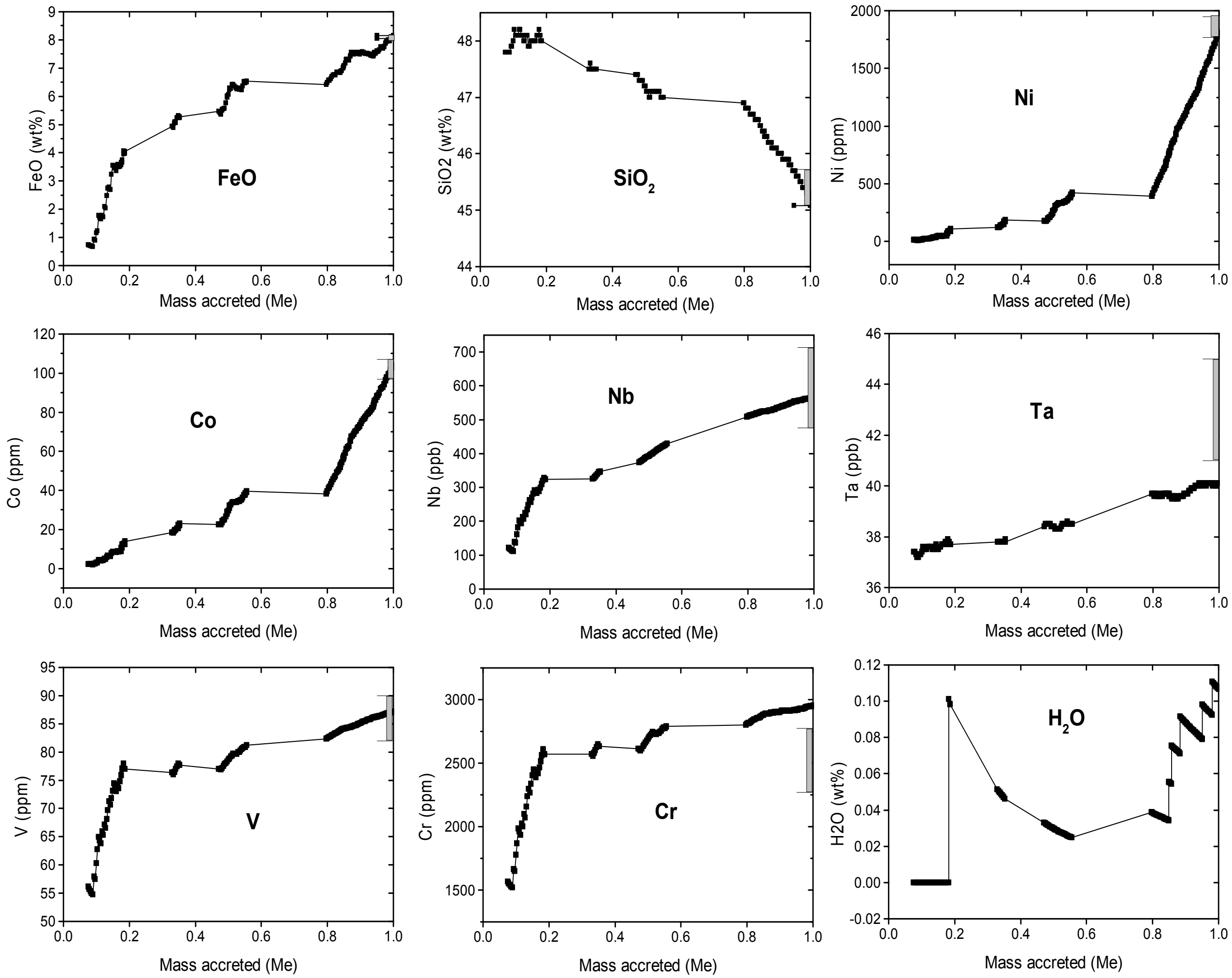


Final core composition: 82 wt% Fe, 5 wt% Ni, 9 wt% Si, 3 wt% O, 48 ppm H

# 4:1-0.5-8: Homogeneous accretion

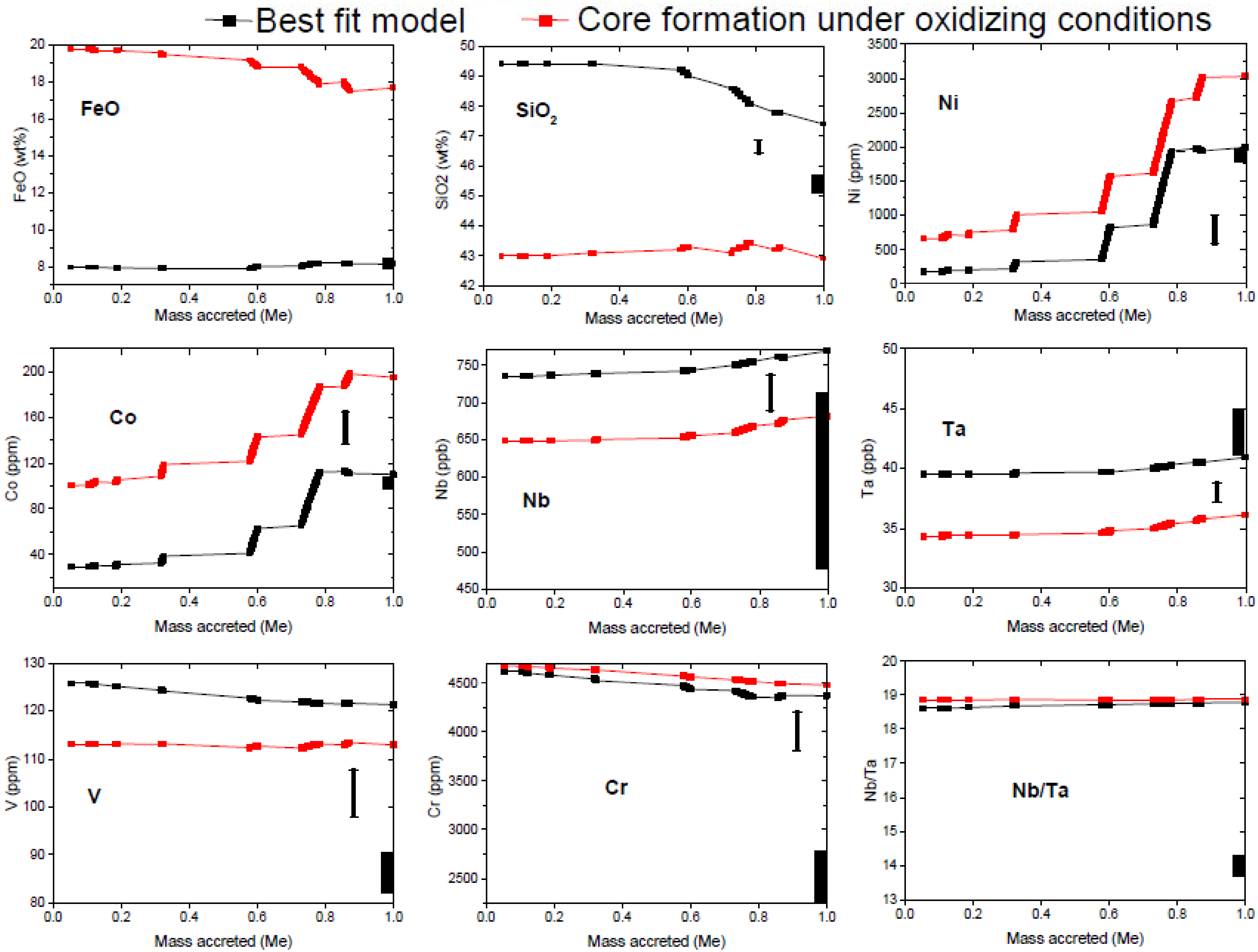

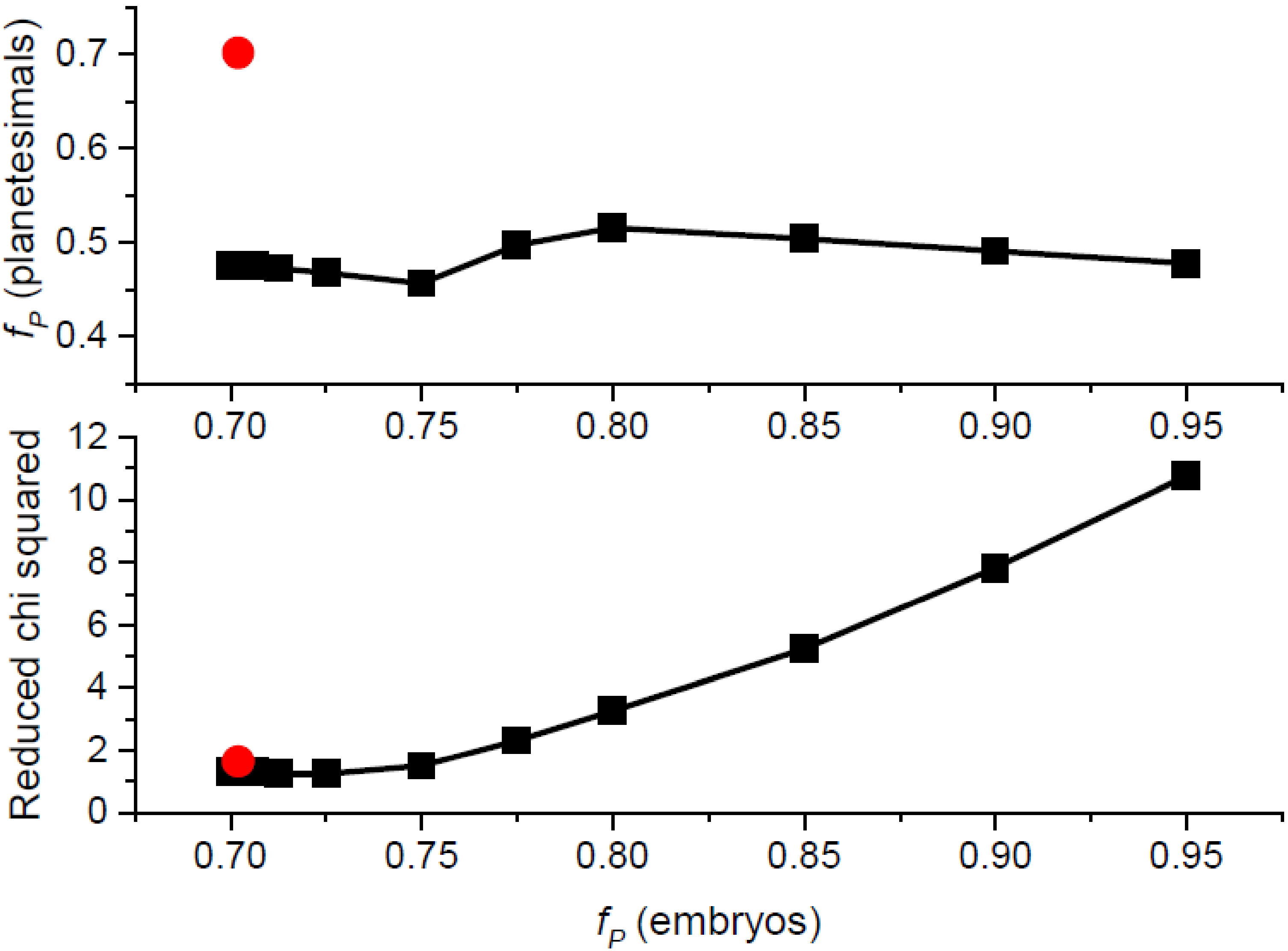

$f_P$ (planetesimals)
0.4
0.5
0.6
0.7
0.70
0.75
0.80
0.85
0.90
0.95
Reduced chi squared
0
2
4
6
8
10
12
0.70
0.75
0.80
0.85
0.90
0.95
$f_P$ (embryos)

# Evolution of mantle compositions of Mercury and Mars based on preferred composition-distance model

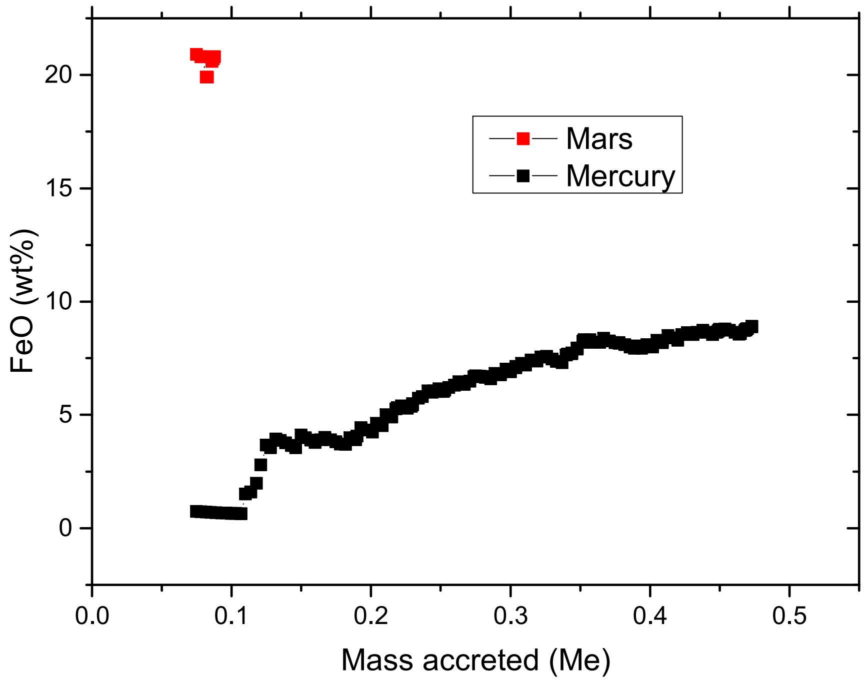


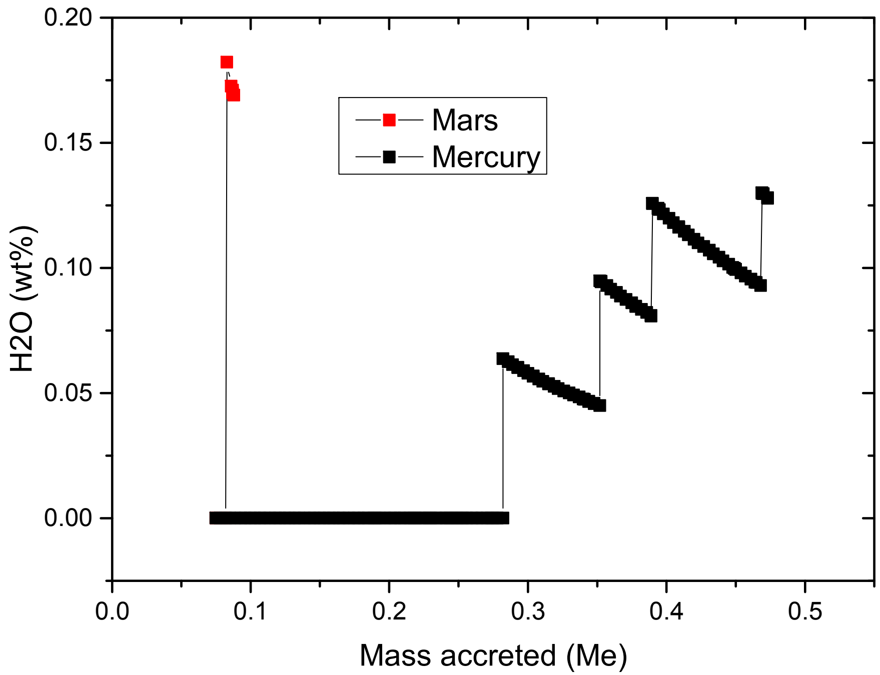


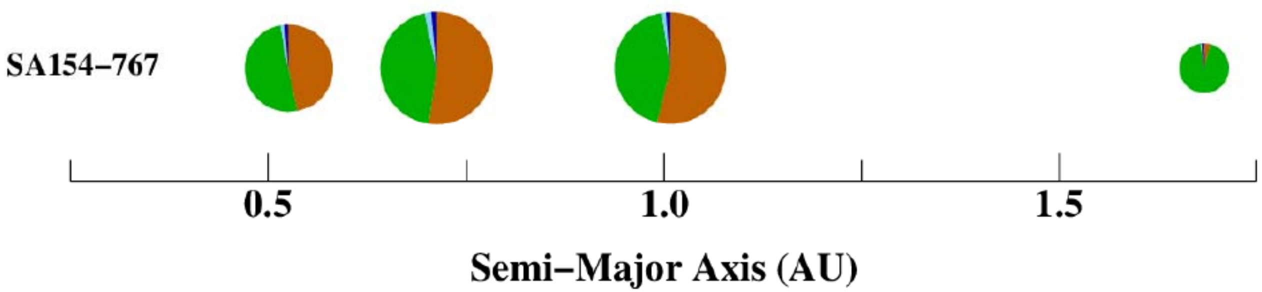

# Constraints on core-formation modeling

Earth-mantle concentrations of the non-volatile siderophile elements:
**Fe, Si, Ni, Co, Nb, Ta, V and Cr + Nb/Ta**

## (FeO contents of mantles of Mars & Mercury)

---

## 2-5 least-squares fitting parameters:

- 1-4 parameters that define the composition of primitive bodies as a function of their heliocentric distances of origin
- Metal-silicate equilibration pressure – as a fraction of a proto-planets's CMB pressure (typically 0.5-0.6).

# Cause of oxidation

- Oxygen fugacities of a solar gas are orders of magnitude more reducing than the intrinsic oxygen fugacities at which the terrestrial planets formed but are consistent with the region of highly-reduced compositions at <1.3 AU postulated here. Thus oxidation is required.

- Due to the inward net flow of material in the solar nebula, ice-covered dust moves inwards from beyond the snow line.
- Inside the snow line, water ice sublimes, adding $H_2O$ to the vapor phase. As temperatures continue to rise and material continues to move inward, $H_2O$-rich vapour reacts with Fe-bearing dust, resulting in oxidation.
- Inward still, vapour is $H_2O$-poor because the products of sublimed water ice have not mixed all the way to the inner-most solar system. Here Fe remains largely free of oxidation.

# Evolution of the concentration of light elements in Earth's core

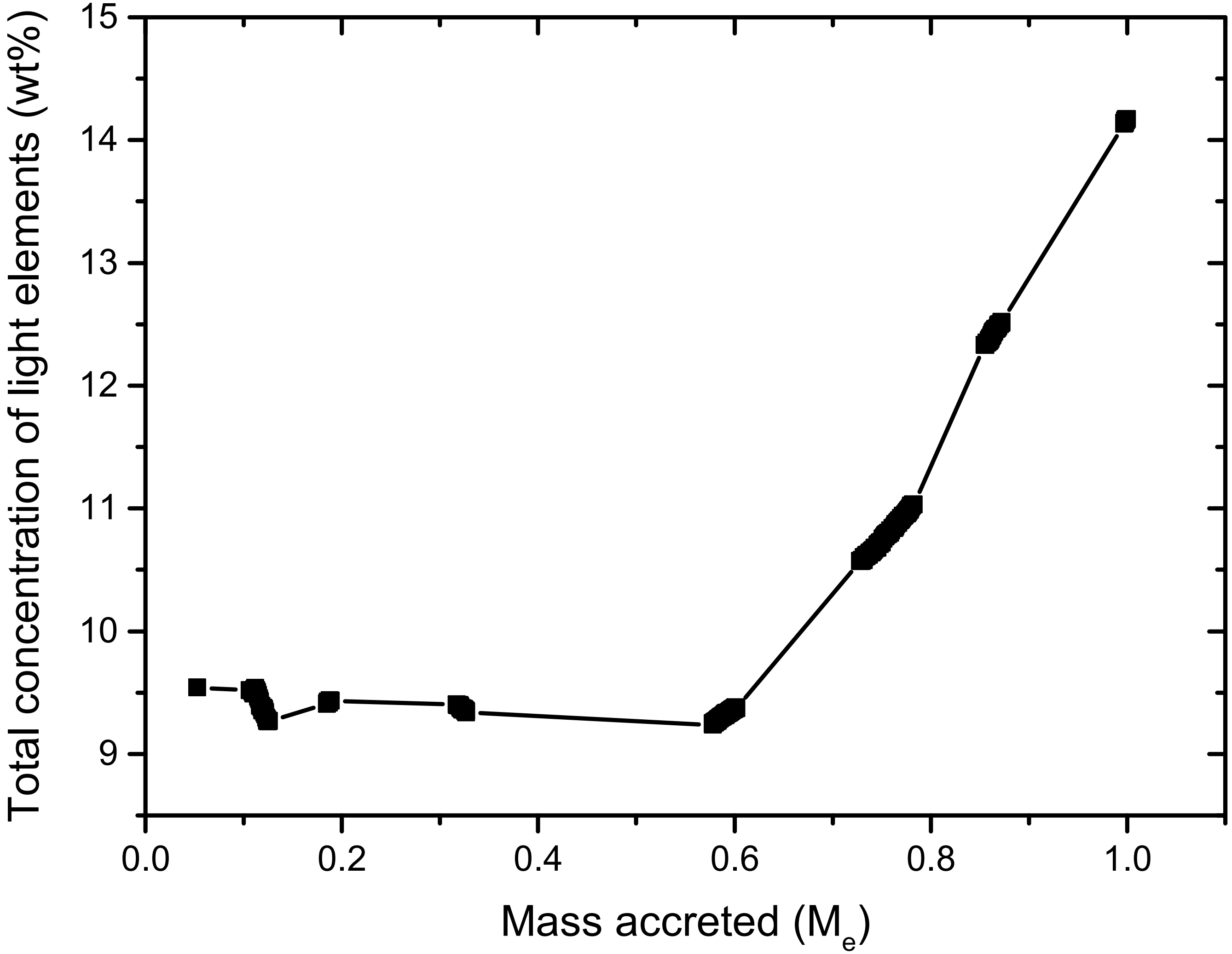

# Tested composition-distance models for primitive bodies

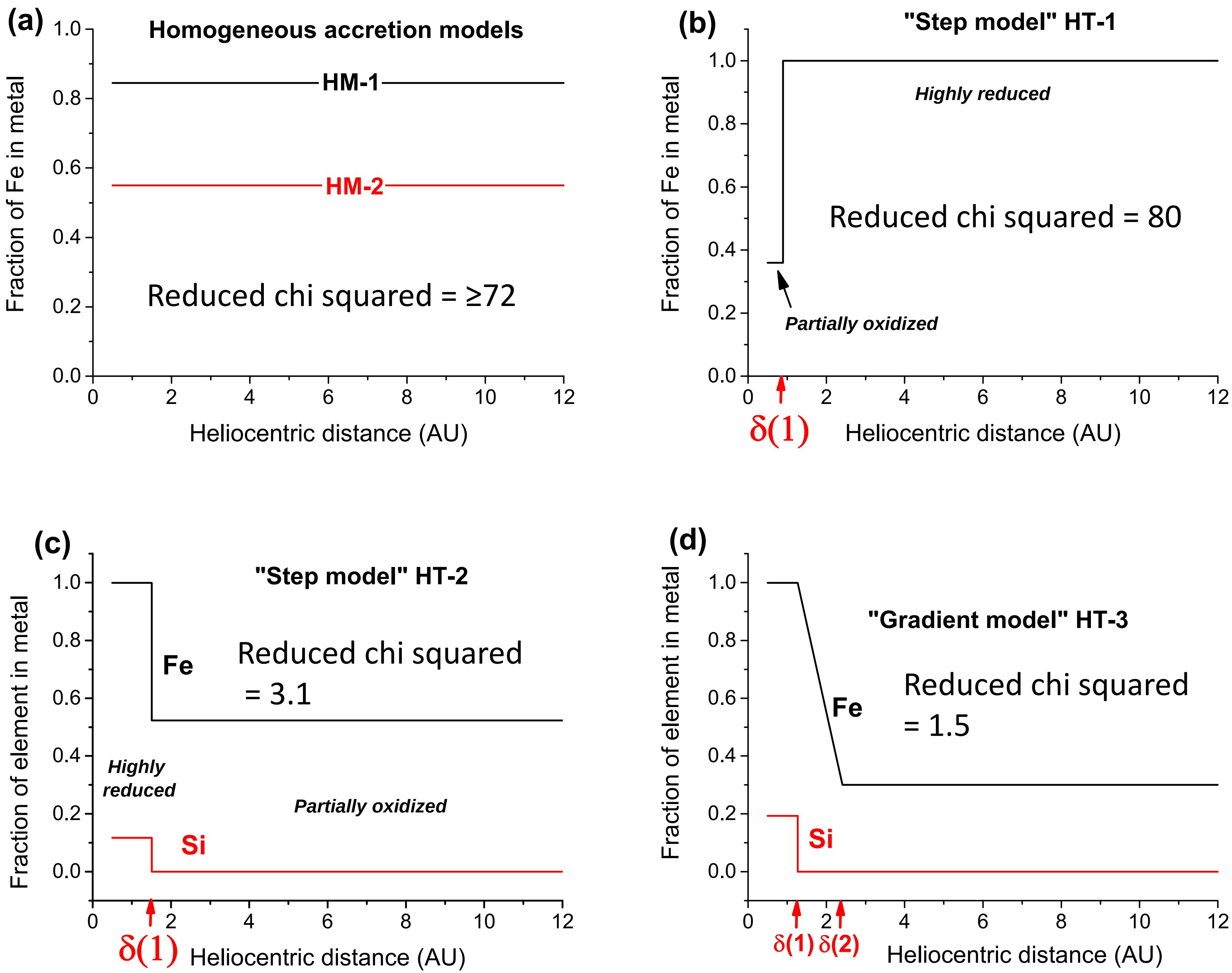

# Lower mantle seismic observations

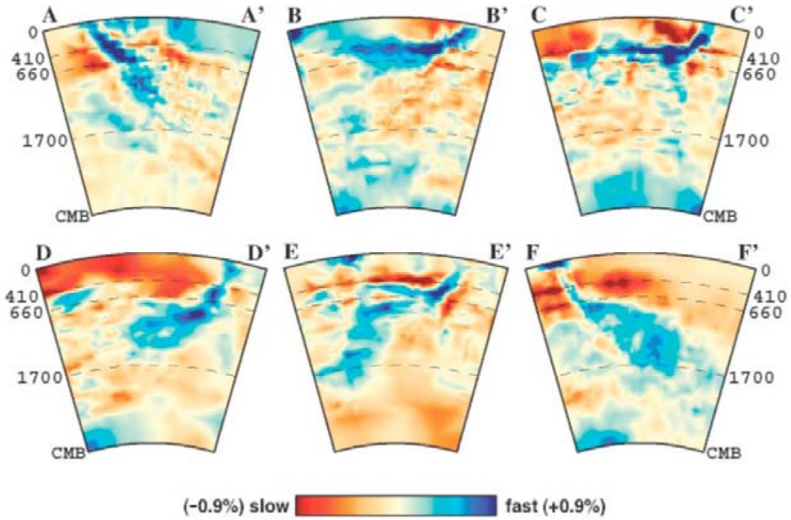


Karason & van der Hilst 2000

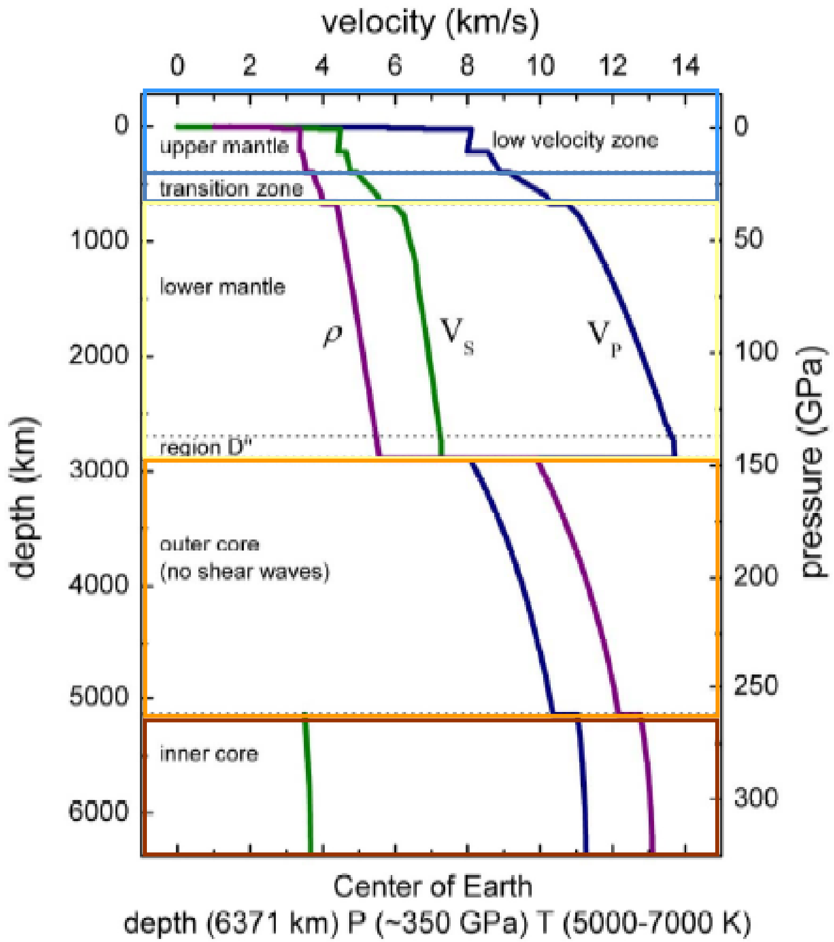


Dziewonski and Anderson 1981

# A peridotitic lower mantle

BSE e.g
McDonough & Sun 1995

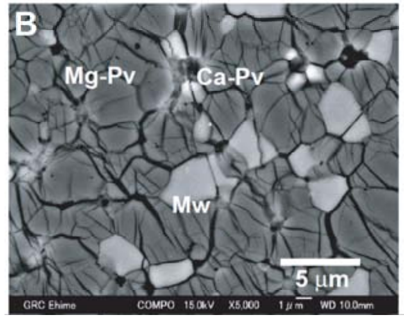


**72 mole % (Mg,Fe)(Al,Si)$O_3$Bridgmanite**

22 mole % (Mg,Fe)O Ferropericlase

6 mole %$CaSiO_3$ Perovskite

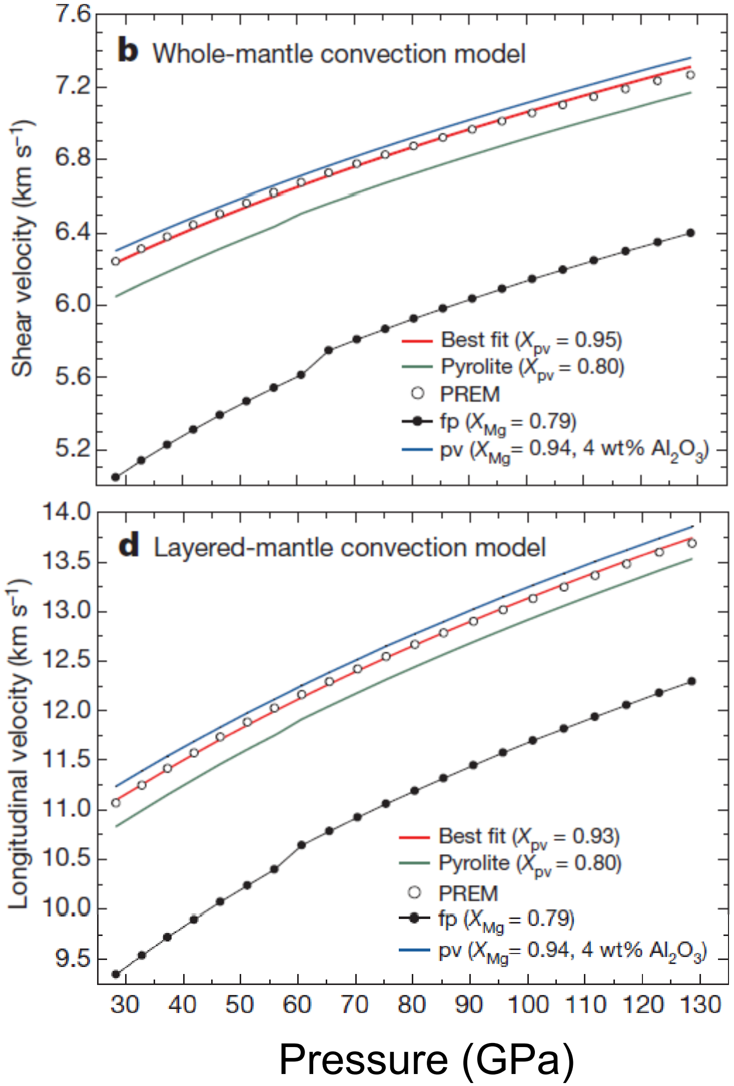


Murakami et al. 2012

# Brillouin scattering

- Laser light interacts with phonons and is scattered with Doppler shifted frequency $\Delta\omega$

$$V_i = \Delta\omega\lambda \,/\, 2n^*\sin(\theta/2)$$

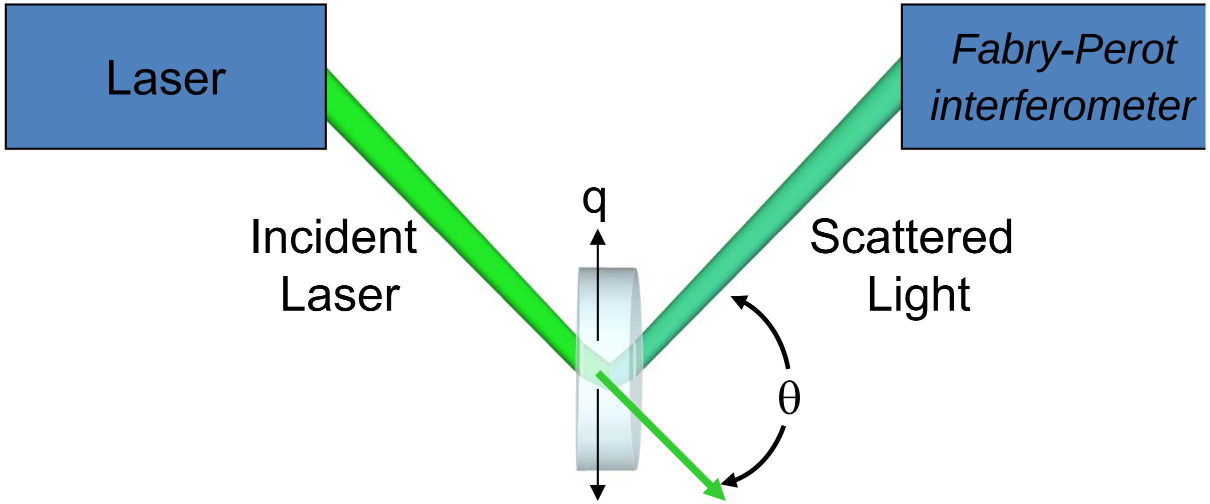


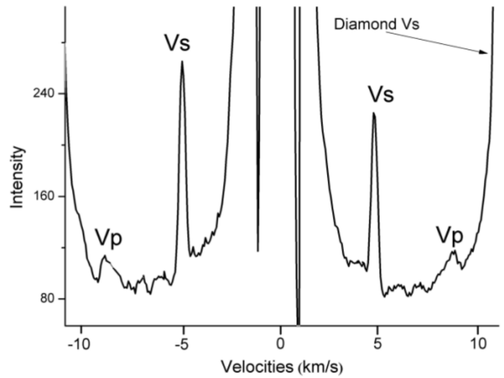

# Diamond anvil cell and Brillouin scattering

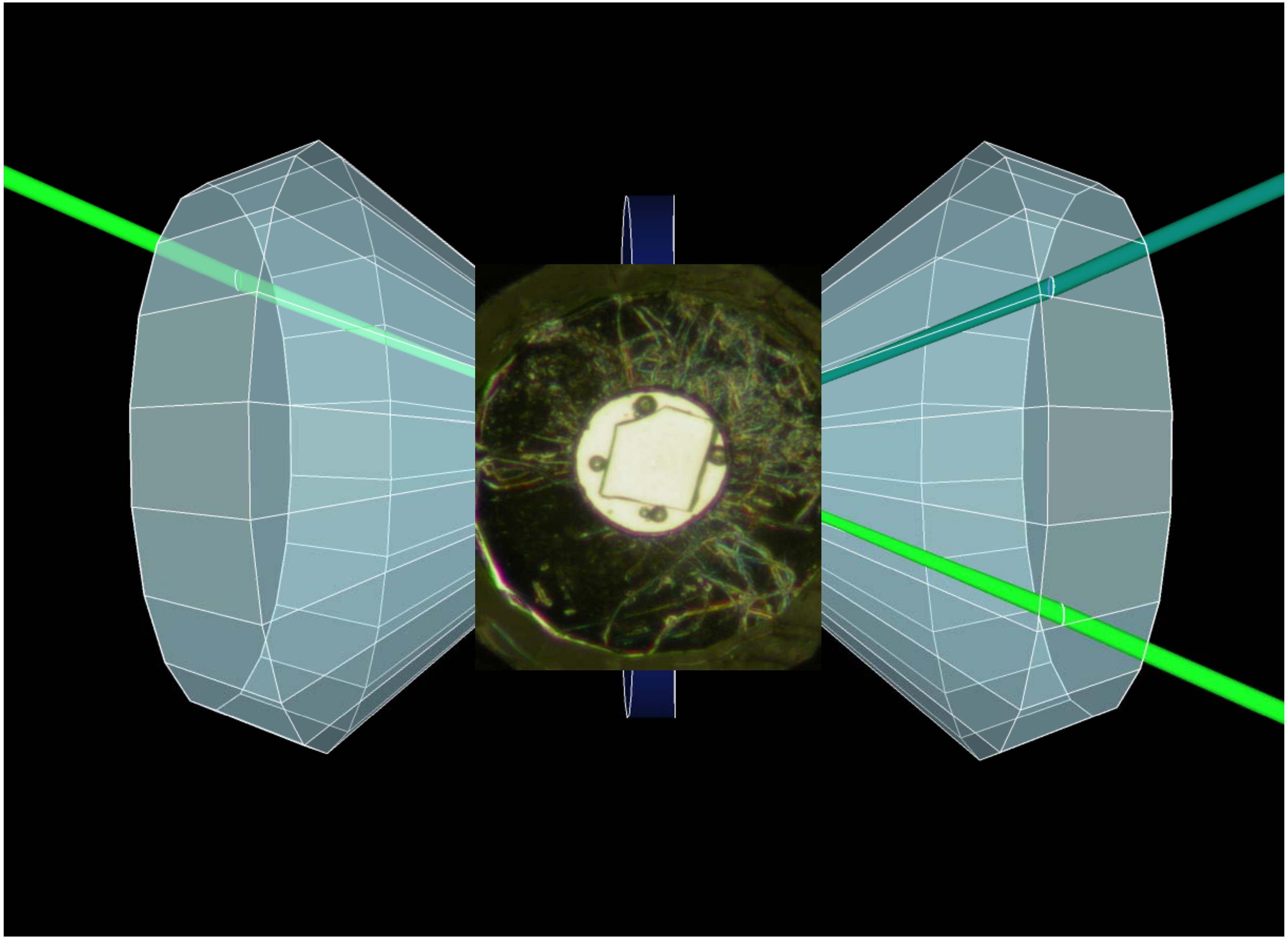

# Brillouin scattering X-ray diffraction lab

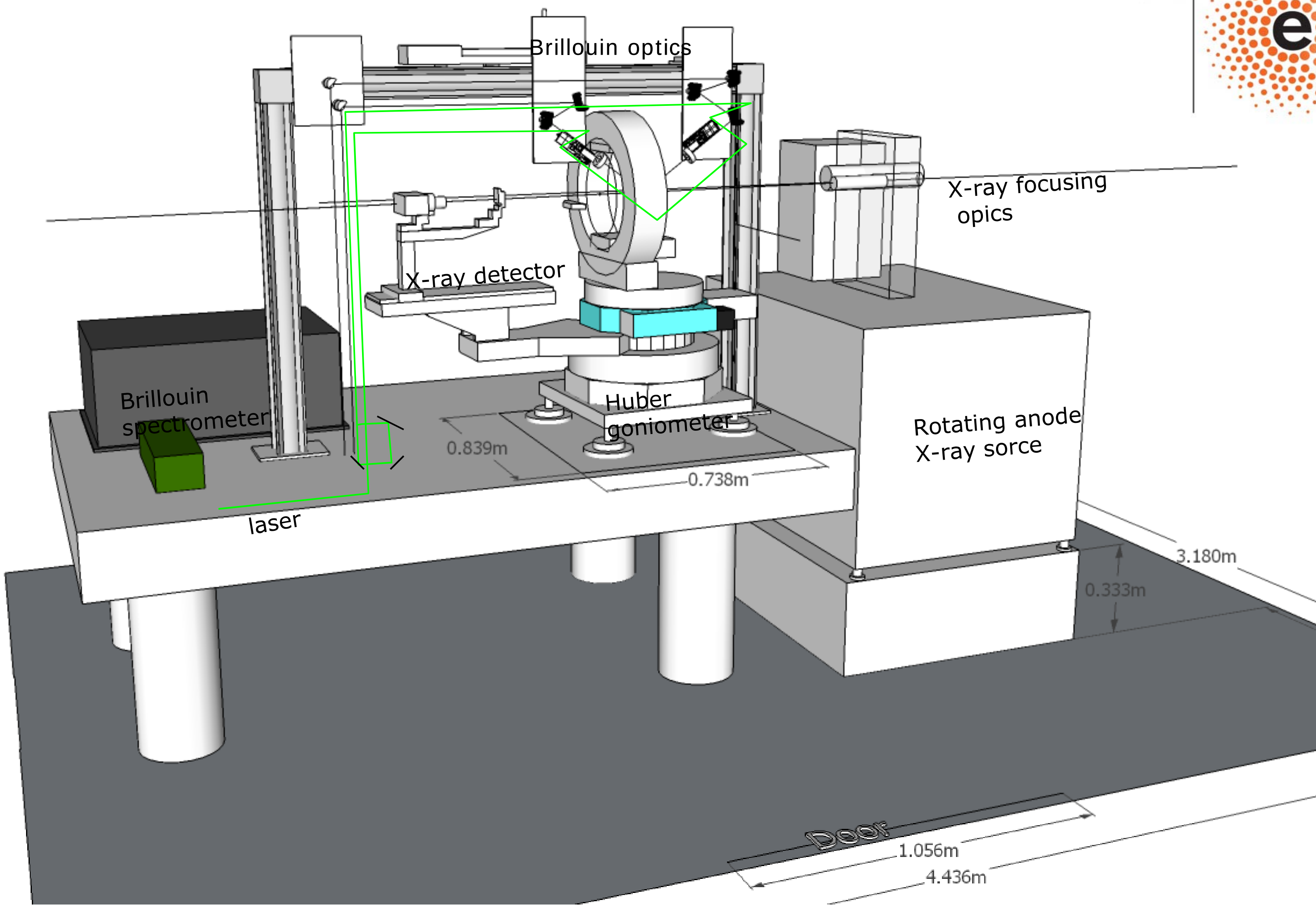

# $MgSiO_3$ Bridgmanite- room temperature

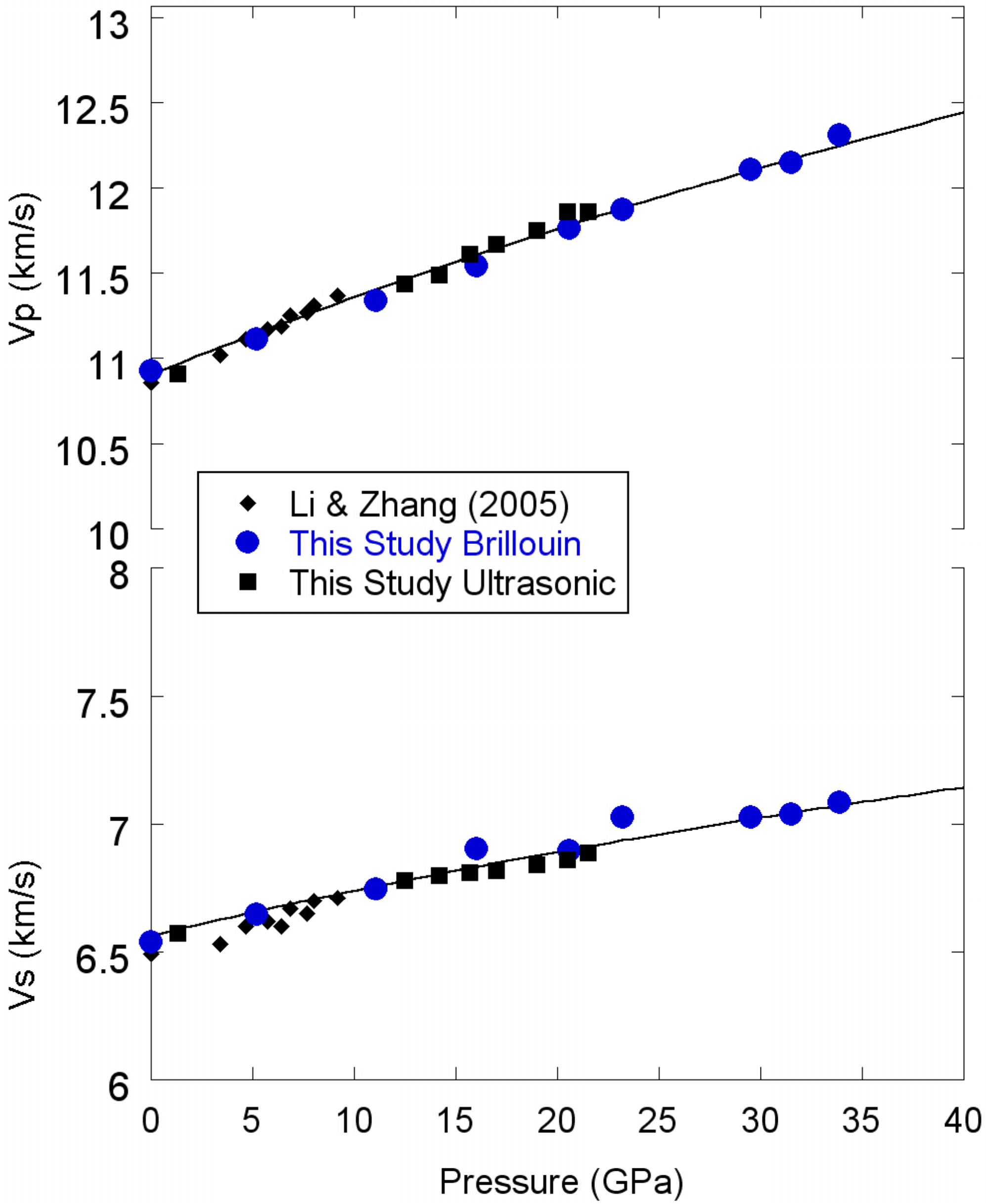

# $(Mg_{0.96}Fe_{0.04})SiO_3$ Bridgmanite- room temperature

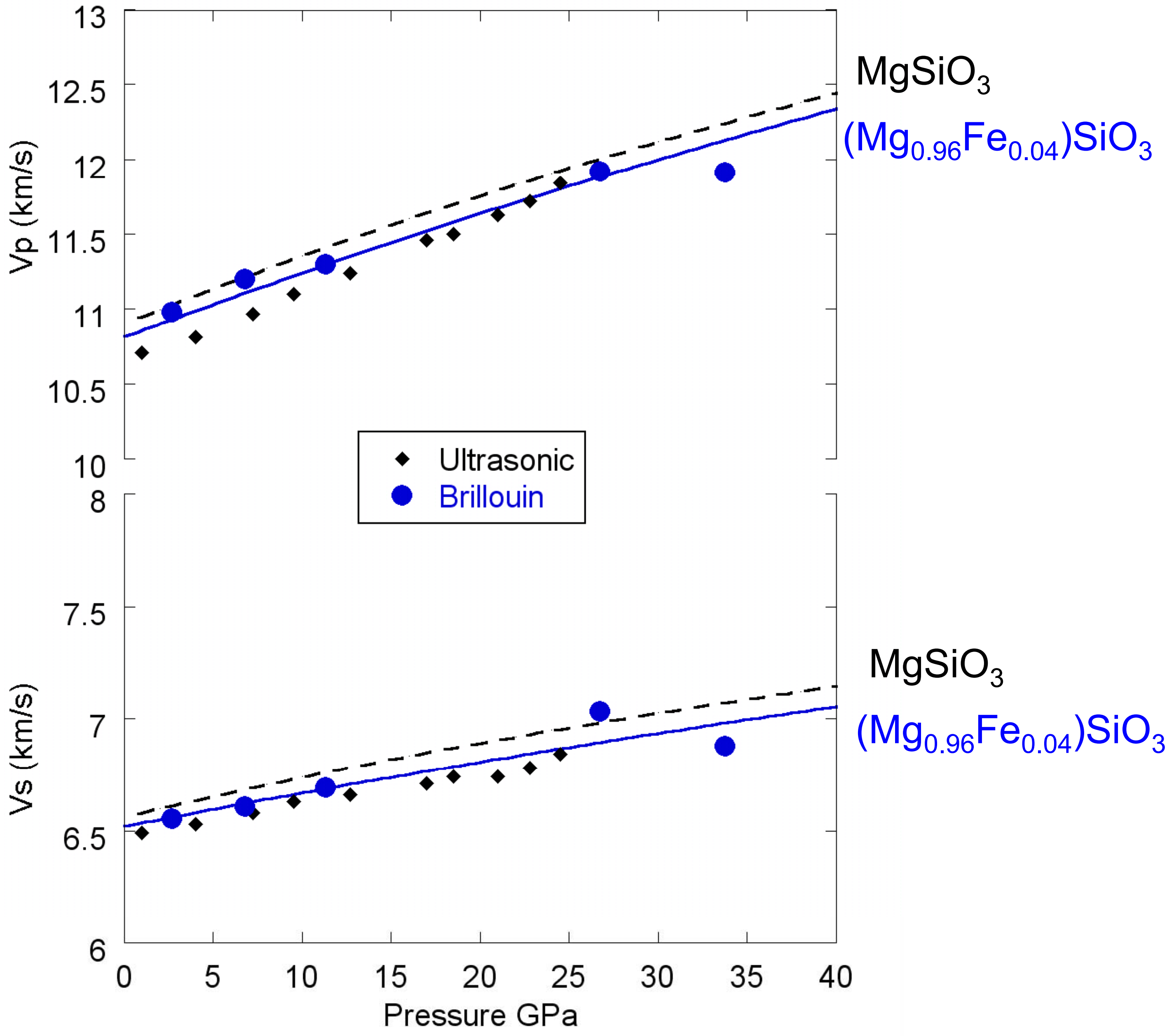

# Ultrasonic measurements at high pressure and temperature

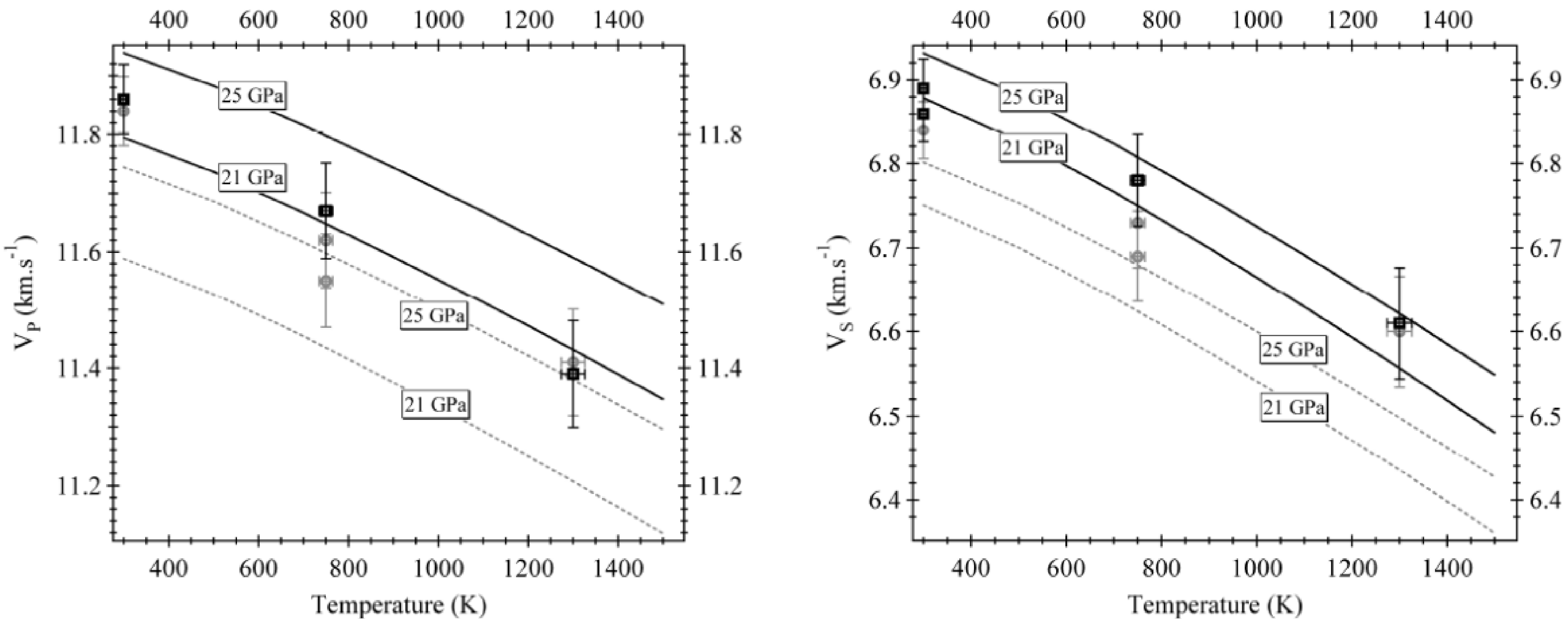


Chantel et al. (2012) GRL 39,L19307

# Thermo-elastic properties of mantle end-members

Thermo-elastic paramaters of the mantle phases used for calculating the sound wave velocities and densities as a function of pressure and temperature in the transition zone and lower mantle.

| Phase | Formula | $V_0$ ($cm^3$/mol) | $K_{T0}$ (GPa) | $K'_{T0}$ | $\theta_0$ (K) | $\gamma_0$ | $q_o$ | $G_0$ (GPa) | $G_0'$ | $\eta_{s0}$ |
|---|---|---|---|---|---|---|---|---|---|---|
| Wadsleyite | $Mg_2SiO_4$ | *4.052* | *169* | *4.3* | *853* | *1.21* | *2* | *112* | *1.4* | *2.6* |
| Wadsleyite | $Fe_2SiO_4$ | *4.28* | *169* | *4.3* | *719* | *1.21* | *2* | *72* | *1.4* | *1.1* |
| Ringwoodite | $Mg_2SiO_4$ | *3.949* | *185* | *4.2* | *891* | *1.11* | *2.4* | *123* | *1.4* | *2.3* |
| Ringwoodite | $Fe_2SiO_4$ | *4.186* | *213* | *4.2* | *652* | *1.26* | *2.4* | *92* | *1.4* | *1.8* |
| Ca-Perovskite | $CaSiO_3$ | *10.98* | *236* | *3.9* | *802* | *1.89* | *0.9* | *157* | *2.2* | *1.3* |
| Stishovite | $SiO_2$ | *1.402* | *314* | *3.8* | *1055* | *1.35* | *2.9* | *220* | *1.9* | *4.6* |
| Perovskite | $MgSiO_3$ | 2.445 | 250.3 | 4.02 | 901 | 1.44 | 1.4 | 176.8 | 1.75 | 2.6 |
| Perovskite | $FeSiO_3$ | 2.54 | 250.3 | 4.02 | 765 | 1.44 | 1.4 | 162.8 | 1.5 | 1.9 |
| Perovskite | $FeAlO_3$ | 2.54 | 220 | 4.1 | 765 | 1.44 | 1.4 | 132 | 1.7 | 1.9 |
| Perovskite | $AlAlO_3$ | 2.549 | 228 | 4.1 | 886 | 1.44 | 1.4 | 157 | 1.7 | 2.8 |
| Periclase | MgO | *1.124* | *161* | *3.9* | *772* | *1.48* | *1.6* | *130* | *2.3* | *2.3* |
| Wüstite | FeO | *1.226* | *149* | *4.9* | *454* | *1.54* | *1.6* | *47* | *0.7* | *0.6* |

values in italics are taken from Stixrude and Lithgow-Bertelloni (2011); values for perovskite are from Boffa Ballaran et al. (2012); Chantel et al. (2012); Kurnosov et al. (in preparation)

# A peridotitic lower mantle

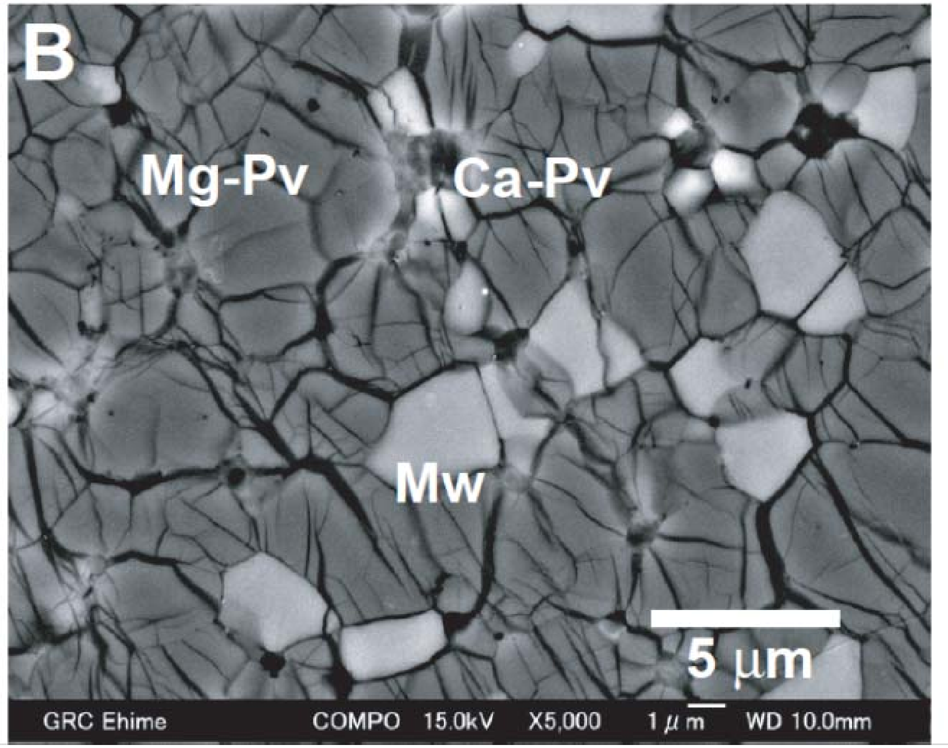


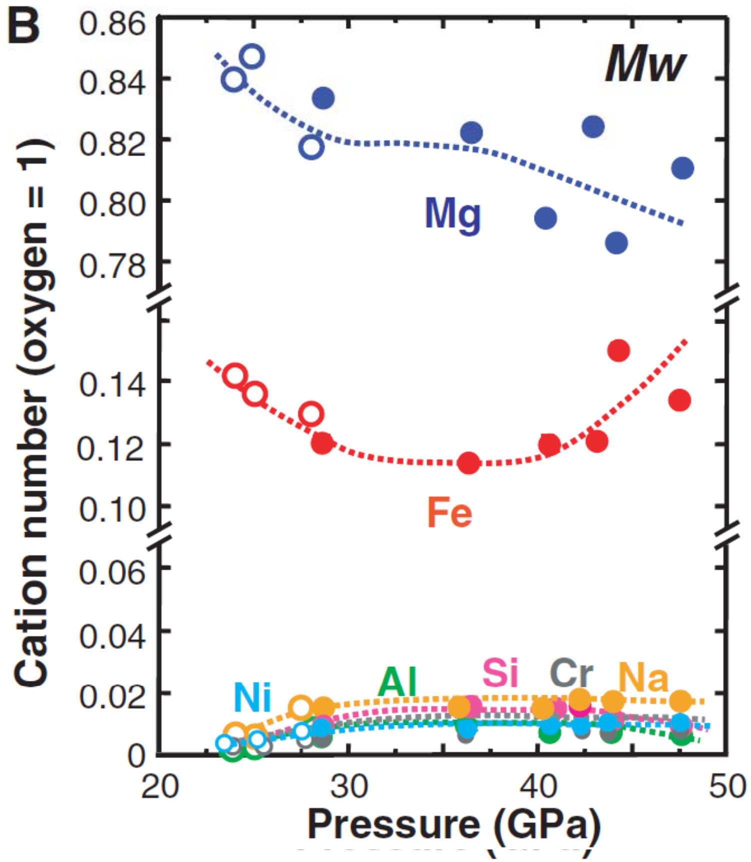


**72 mole % (Mg,Fe)(Al,Si)$O_3$Bridgemanite**

22 mole % (Mg,Fe)O Ferropericlase

6 mole %$CaSiO_3$ Perovskite

Irifune et al. 2010

# Fe and Mg exchchange between Bridgmanite and ferropericlase

$$[K_D = (Fe/Mg)_{Mg\text{-}Pv}/(Fe/Mg)_{Mw}]$$

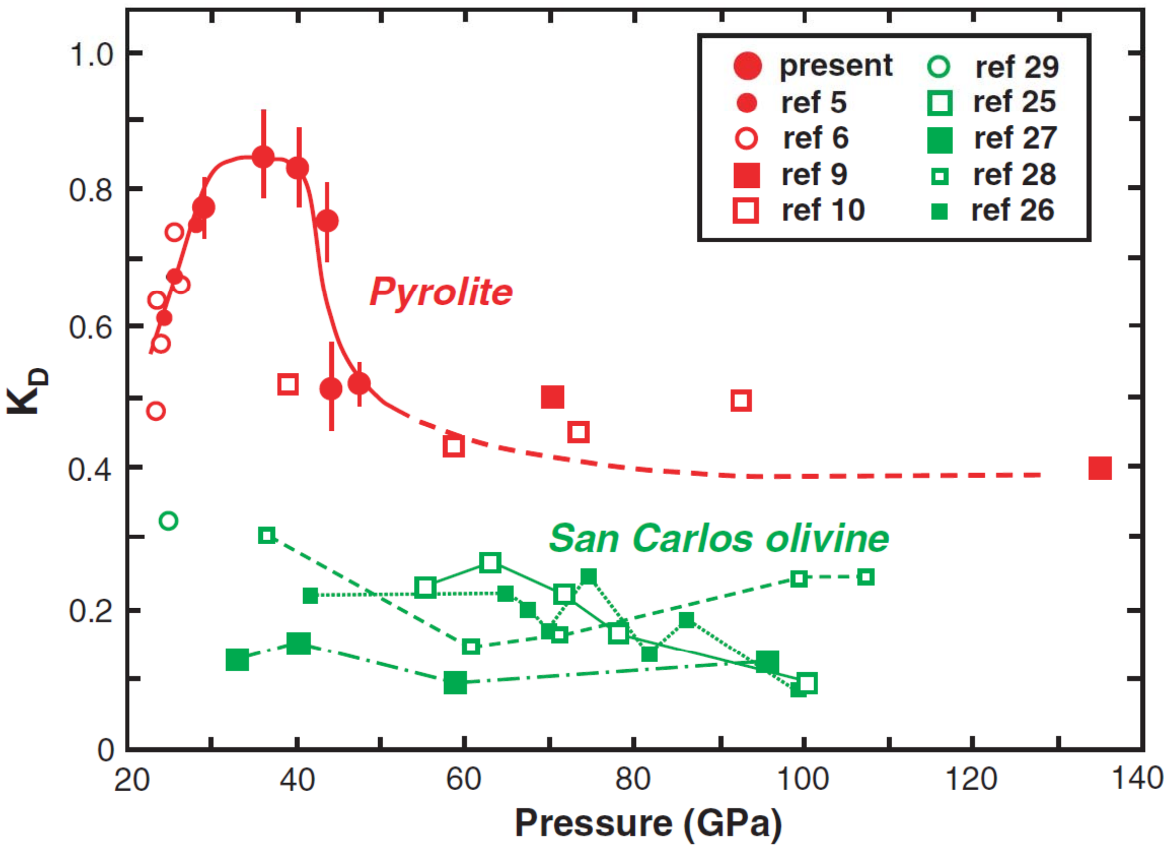


Irifune et al. 2010

# Mineral-physics model for a BSE deep mantle

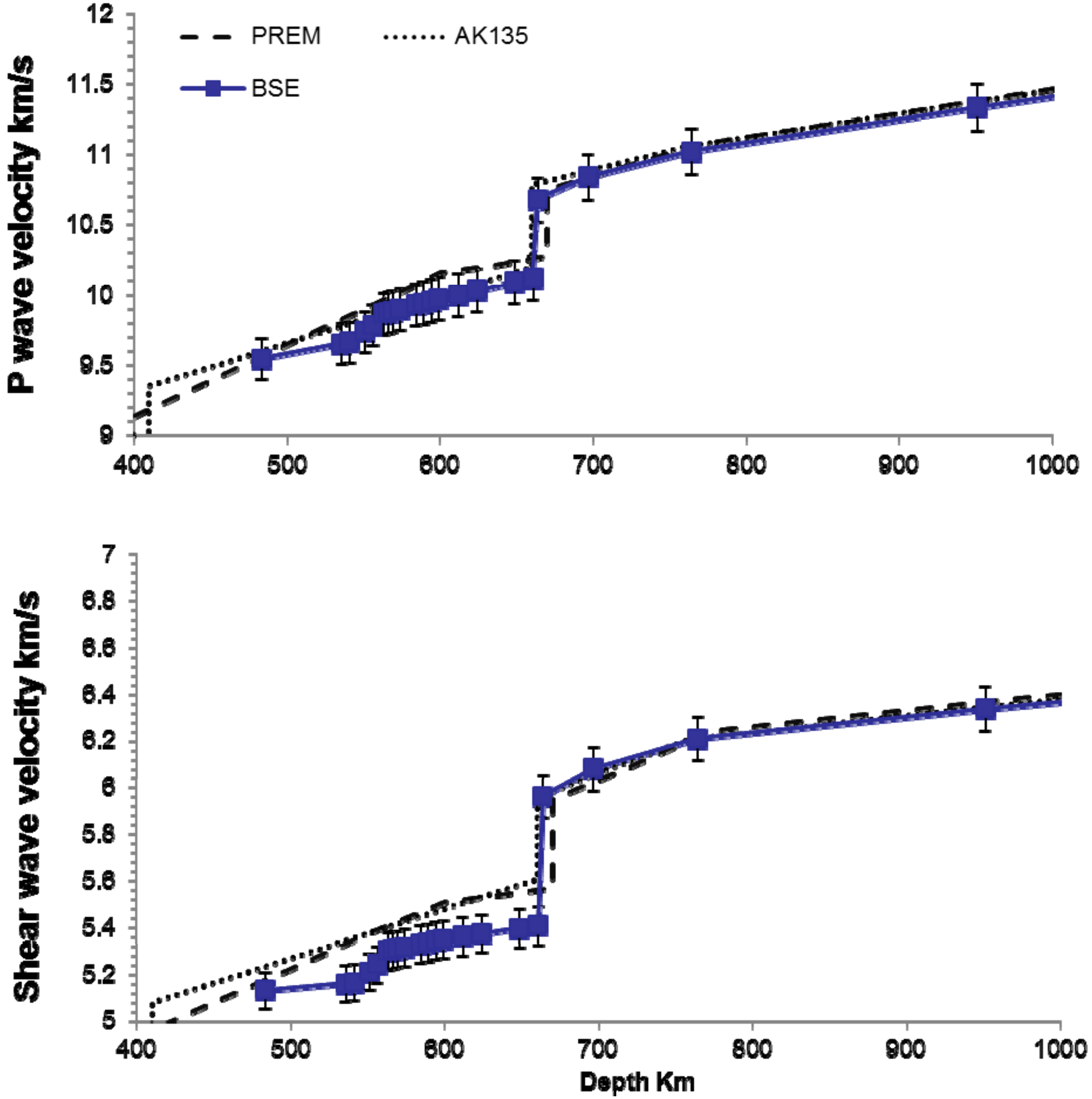

# Influence of Fe-Mg exchange

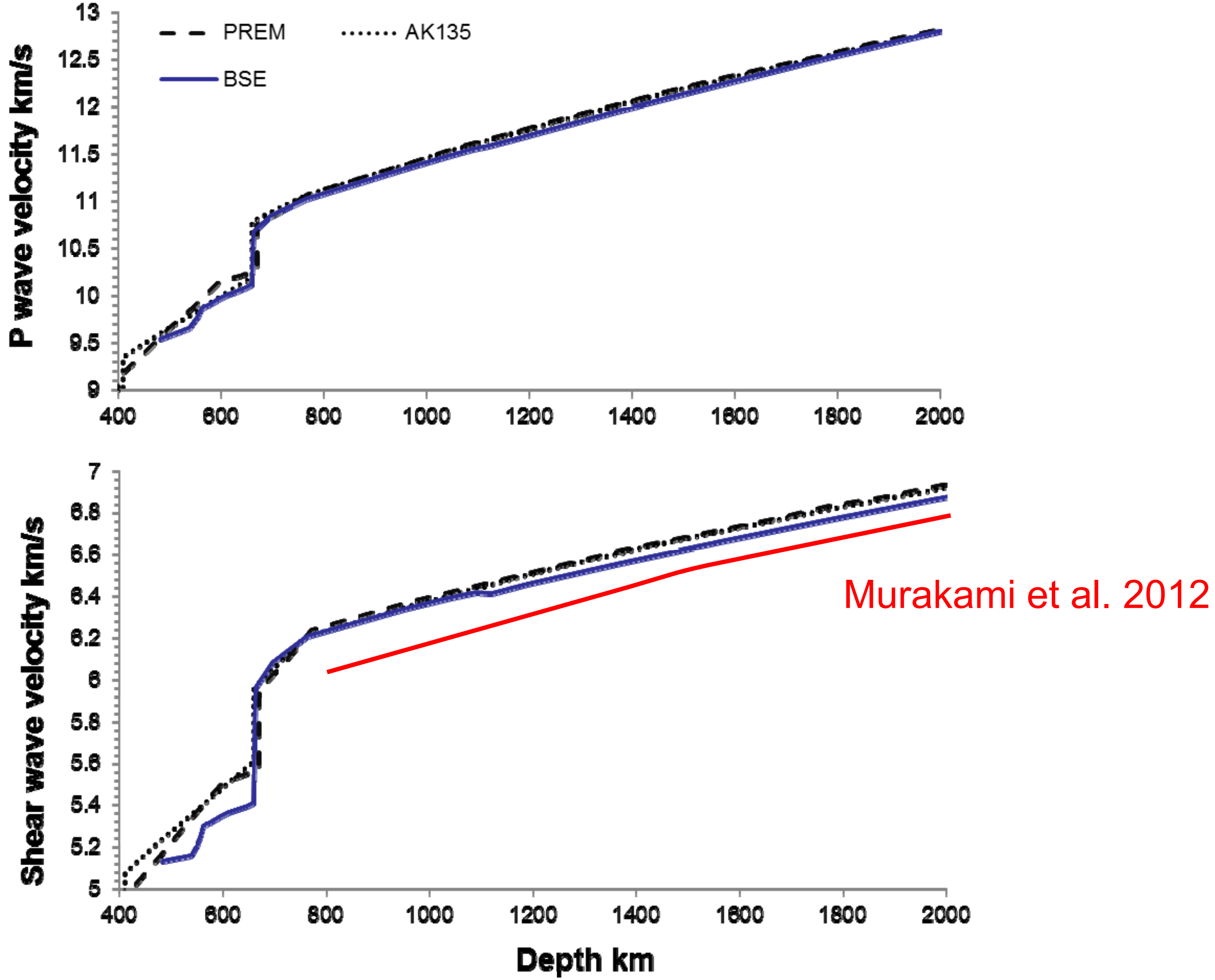

# High ferric iron in Bridgmanite

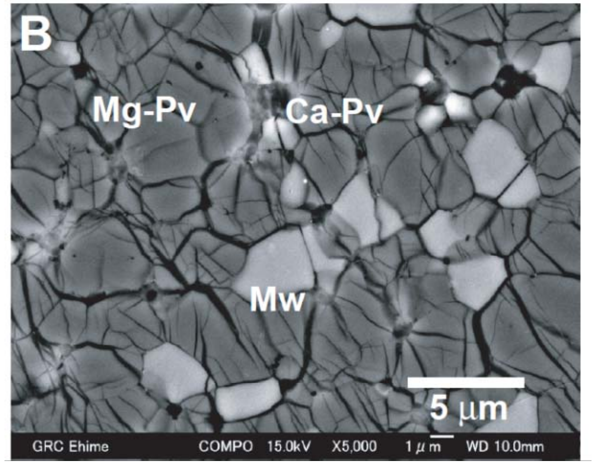


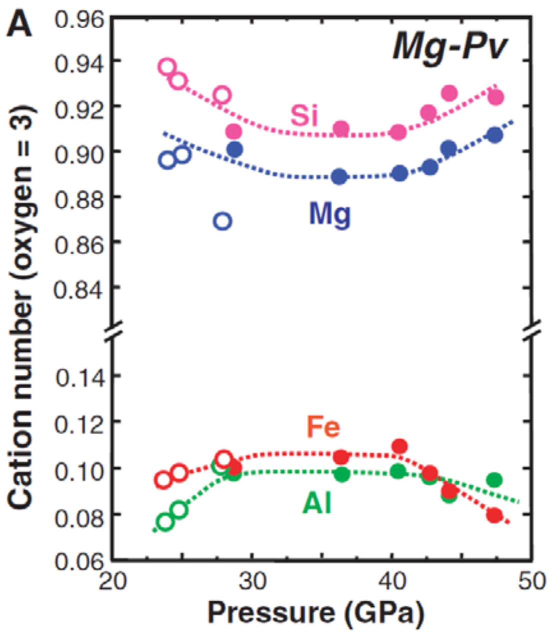


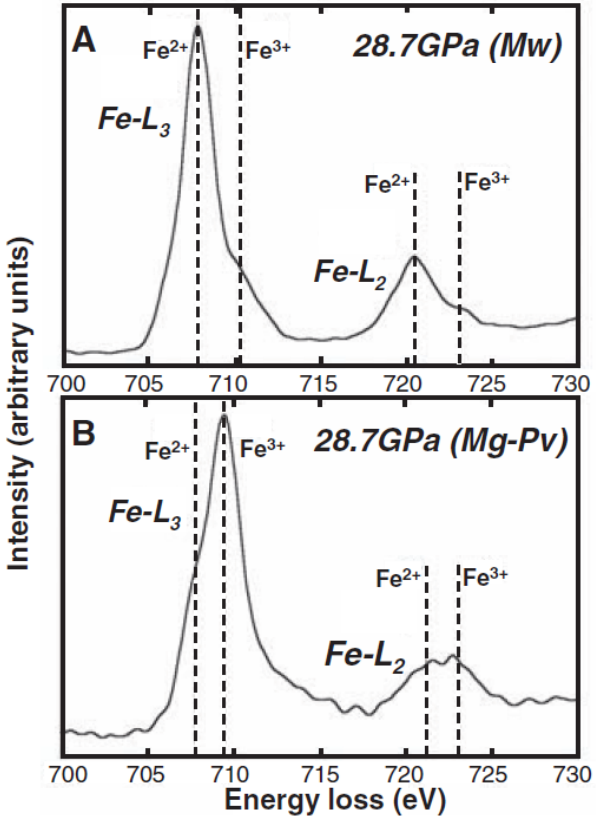


Irifune et al. 2010

Fe3+/TFe

# $Fe^{3+}$ content of Bridgmanite in equilibrium with Fe metal

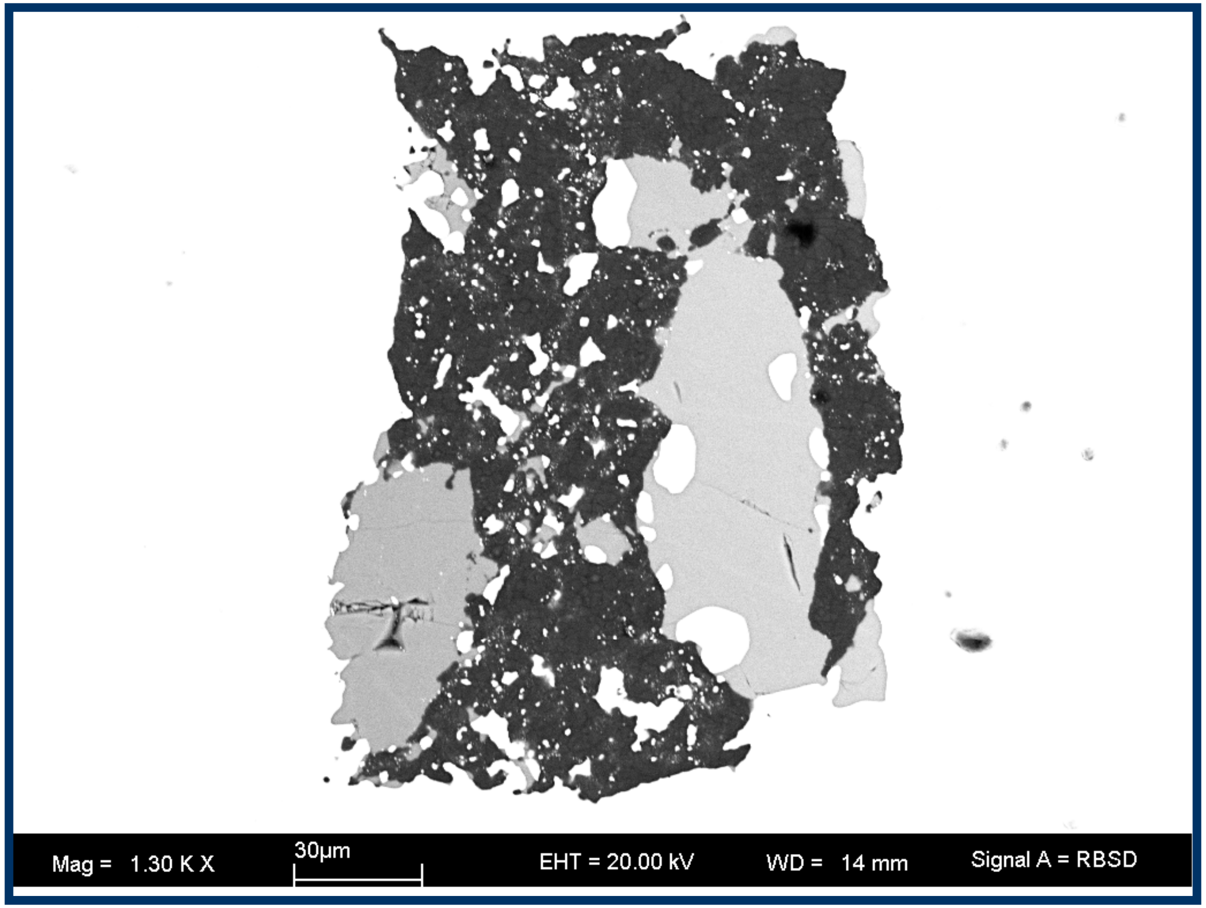

# FeO Disproportionation- constant BSE bulk oxygen

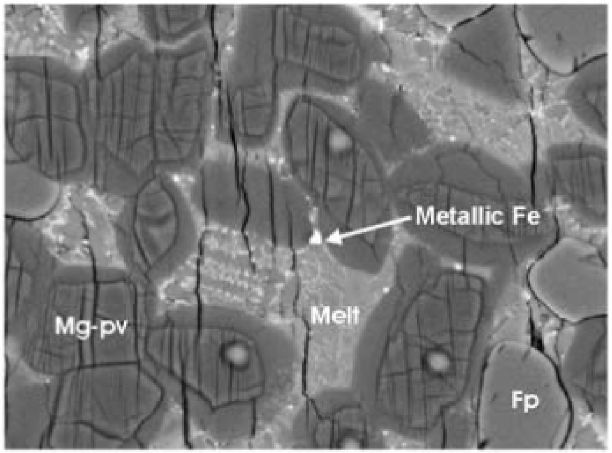


$$3FeO = Fe^0 + Fe_2O_3$$

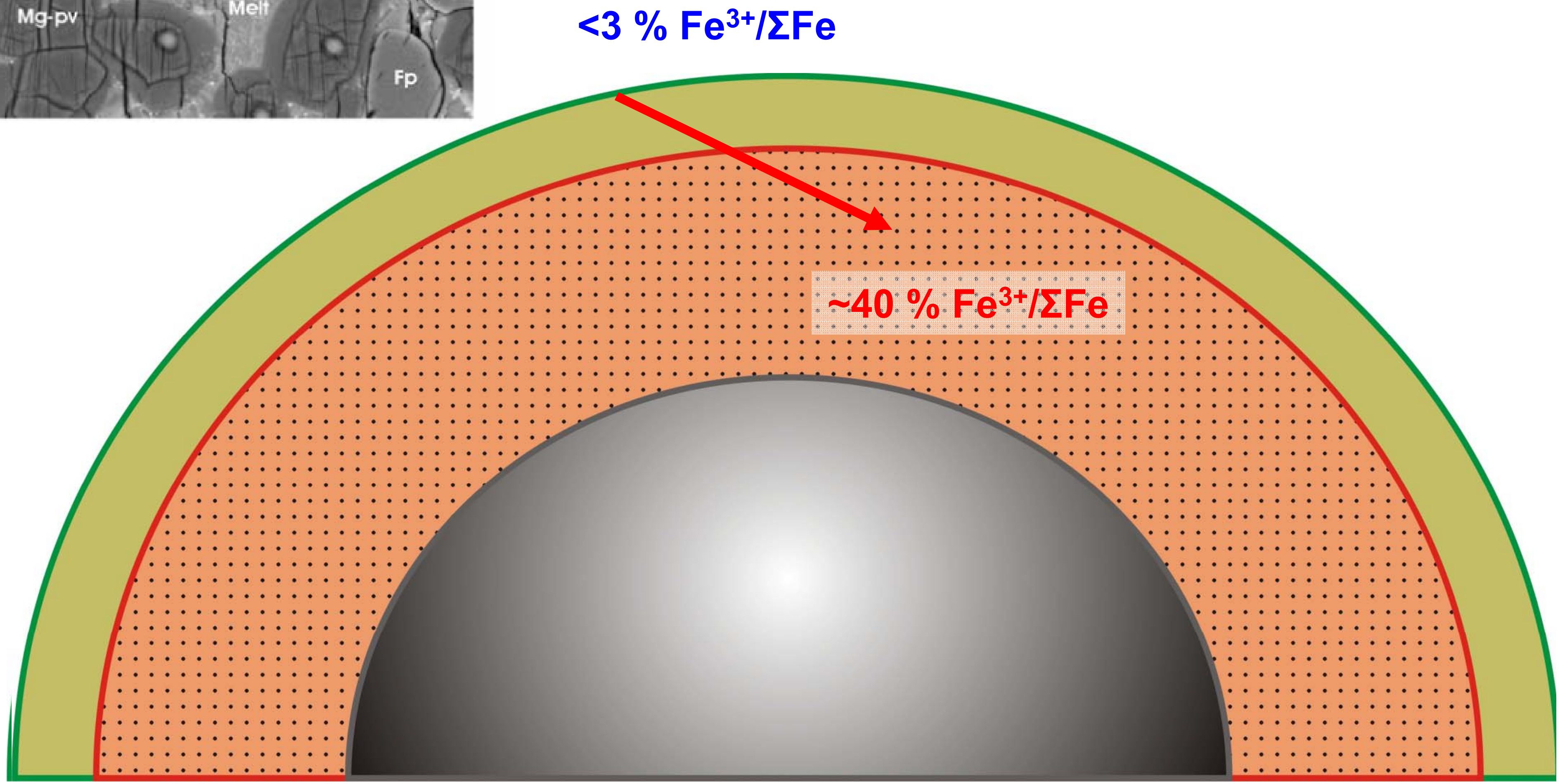

# Mineral physics model with constant BSE bulk oxygen

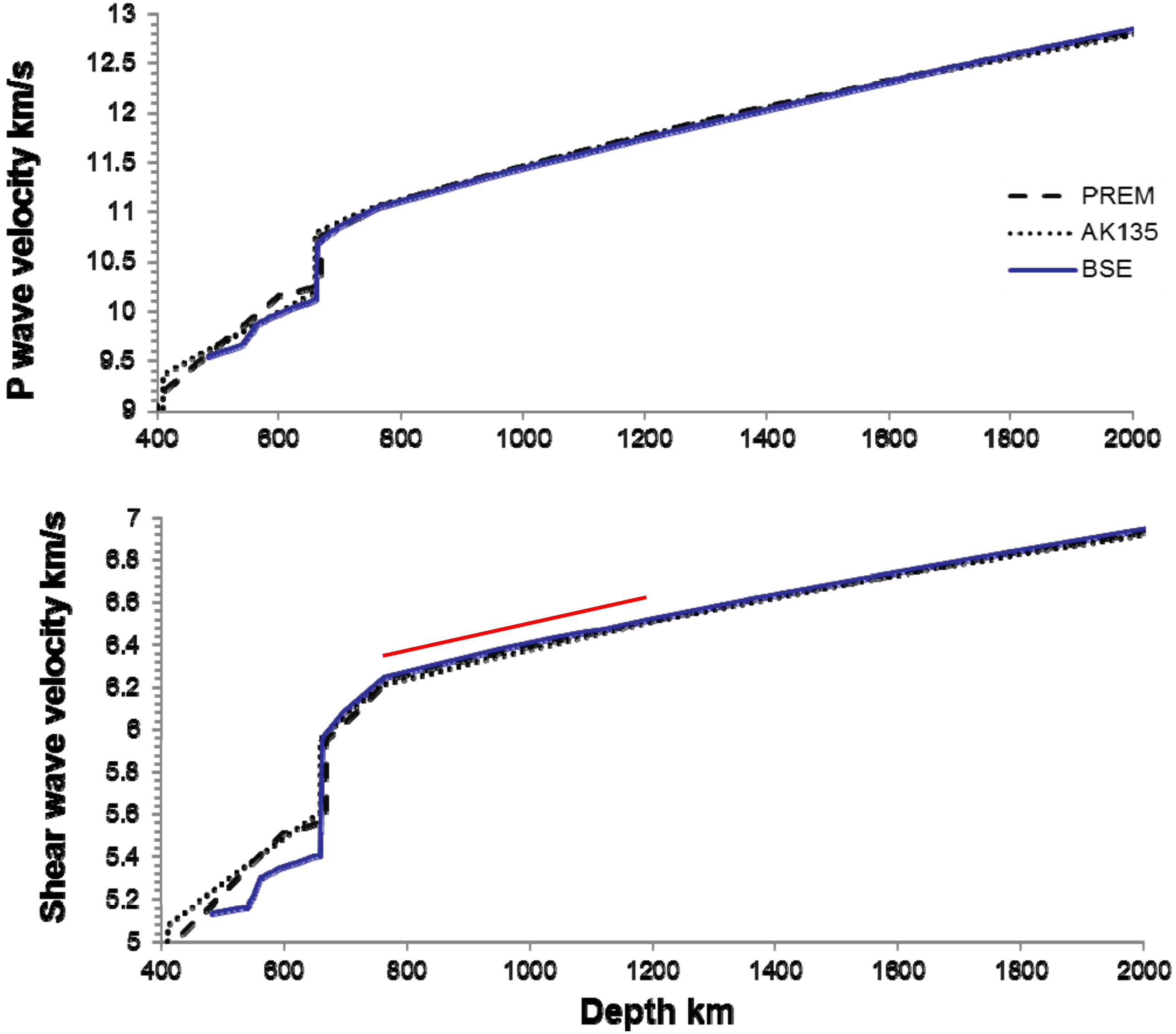

# Summary

- This model does not include Al in perovskite- however previous ultrasonic measurments indicate a limited influence which is currently being tested with Brillouin measurments.

- Vs and Vp estimated for a  BSE composition mineral assemblage in the top 1000 km of the lower mantle match seimsic observations.

- Seismic properties of LLSVPs do not match Fe enrichment in a perovskite dominated mineral assemblage.

# Conclusions

- Combining N-body accretion and core formation modeling provides new constraints on both processes.

- Accretion of Earth and Venus was heterogeneous

- For Earth, Mars and Venus, excellent results are obtained when embryos and planetesimals that form close to the Sun, at <1-1.5 AU, are highly reduced and bodies that form further from the Sun are partially- to fully-oxidized. Other composition-distance models fail badly.

- $H_2O$-bearing bodies in the SA154_767 model originate at >8.5 AU and result in ~1000 ppm $H_2O$ in the mantle

- Results are based on impactor cores equilibrating completely, but with a very limited fraction of a proto-planet’s mantle, at average pressures of 50-60% of CMB pressures.

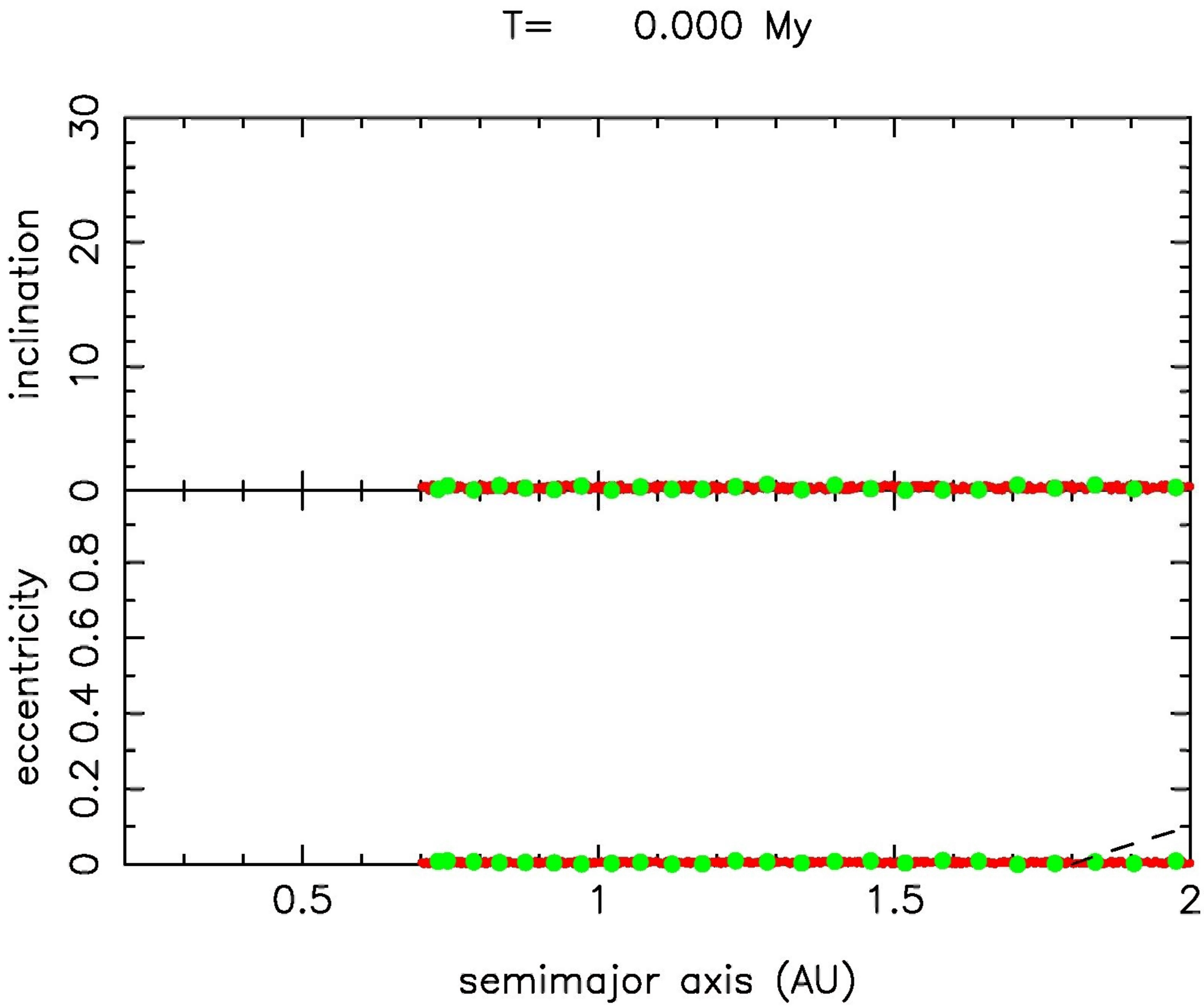

T= 0.000 My
inclination
0
10
20
30
eccentricity
0
0.2
0.4
0.6
0.8
0.5
1
1.5
2
semimajor axis (AU)

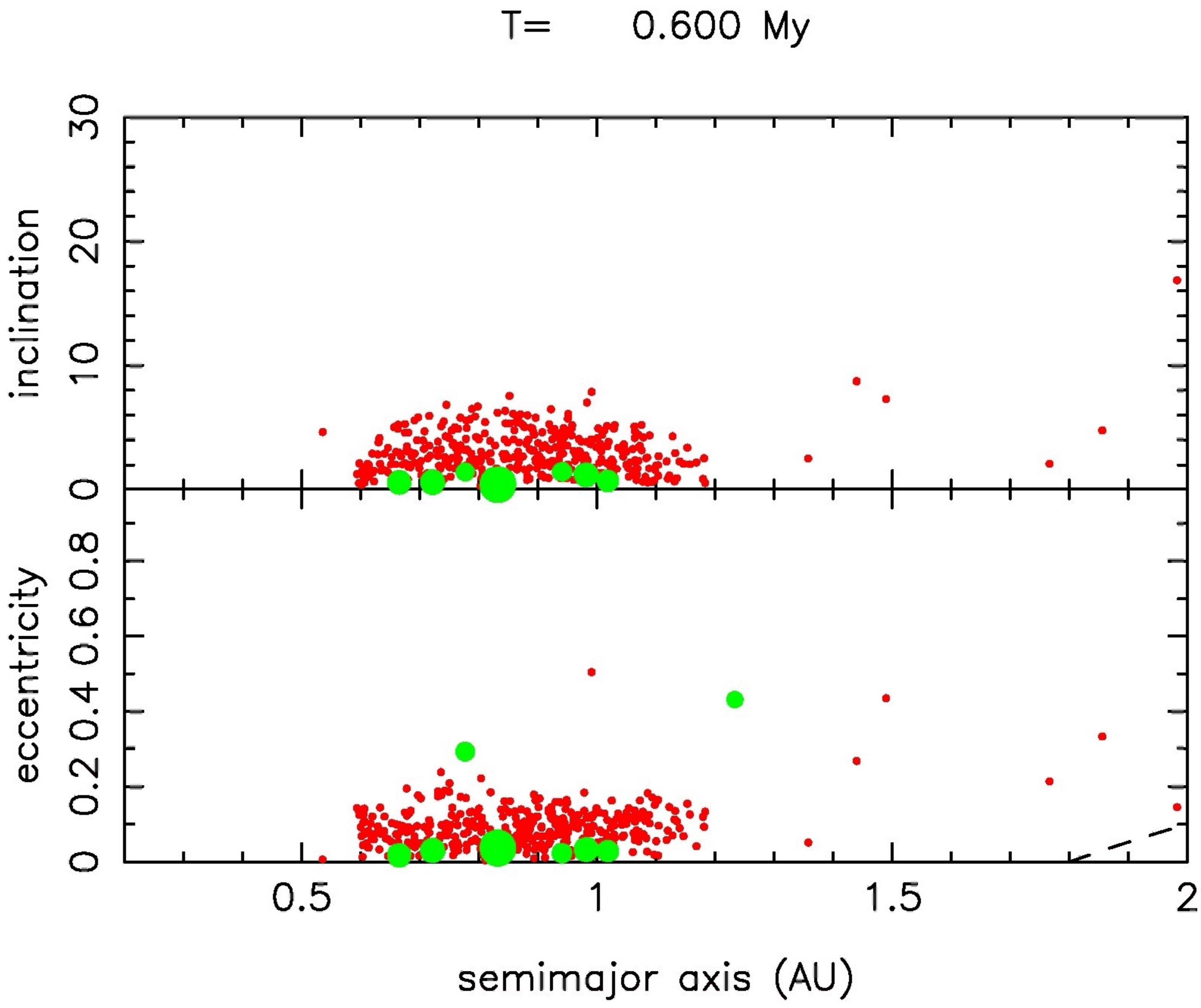

T= 0.600 My
inclination
eccentricity
semimajor axis (AU)
0
10
20
30
0
0.2
0.4
0.6
0.8
0.5
1
1.5
2

# Accretion, heating & metal delivery by impacts

## Core formation and accretion are multistage processes that cannot be separated

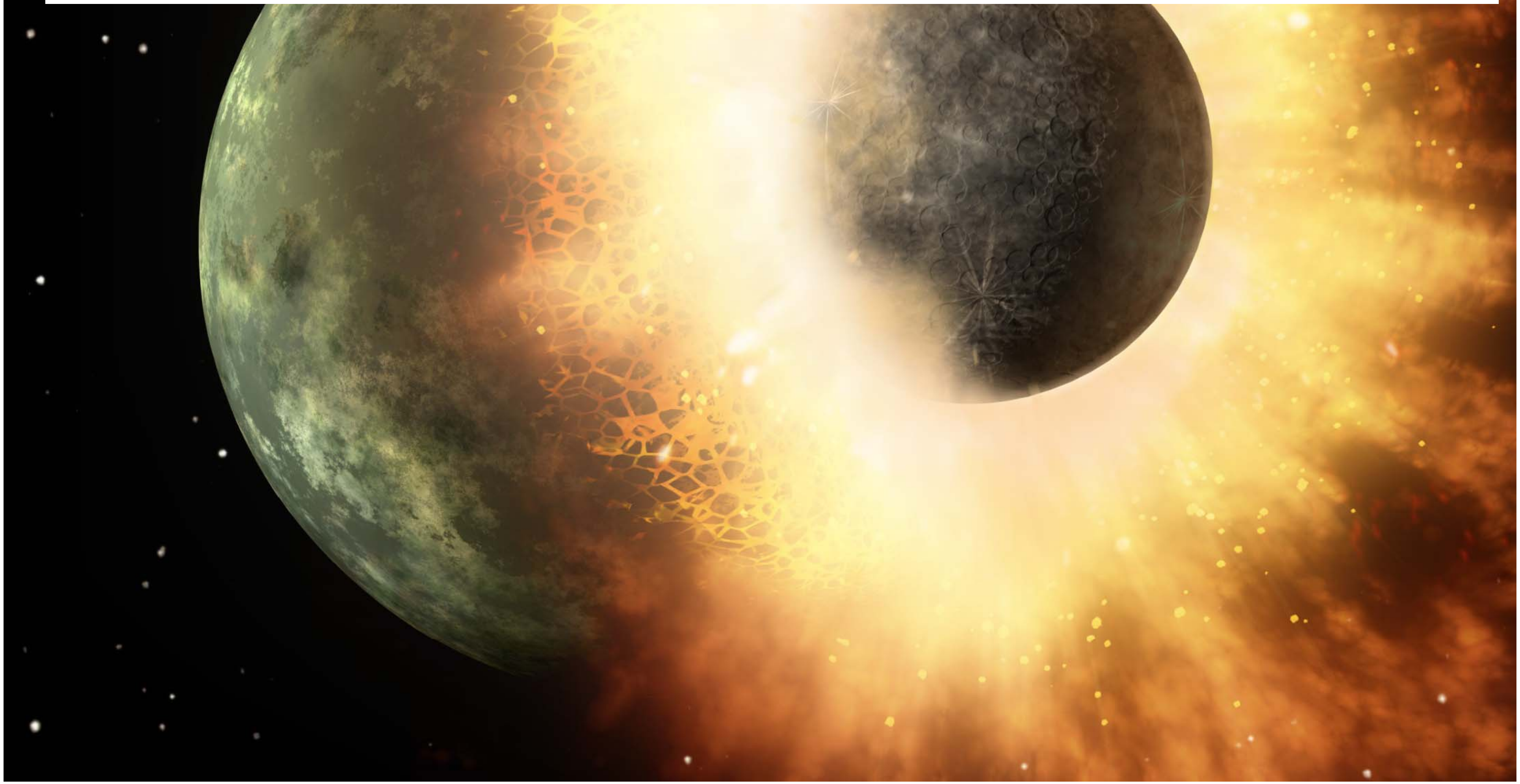

# Grand Tack accretion model

- Classical models (e.g. O'Brien et al 2006) consistently result in a model Mars that is too massive
- The Grand Tack model (Walsh et al., 2011) is based on the inward and then outward migration of Jupiter and Saturn that truncates the planetesimal disk at ~1 AU and results in a realistically small mass for Mars.

# Modeling planetary accretion

- Late stage accretion of terrestrial planets is modeled using "**N-body simulations**". The "Grand Tack" model (Walsh et al., 2011) has been especially successful in reproducing the small size of Mars.

- Start with ~**<u>40 embryos</u>** (0.07 $M_e$) and ~**<u>1500 planetesimals</u>** (0.0003-0.0035 $M_e$), initially dispersed between 0.7 AU and 13 AU, and collide/accrete to form larger bodies.
- ***Combine core-mantle differentiation with N-body accretion models***

# Accretion history of Grand Tack simulation SA154_767

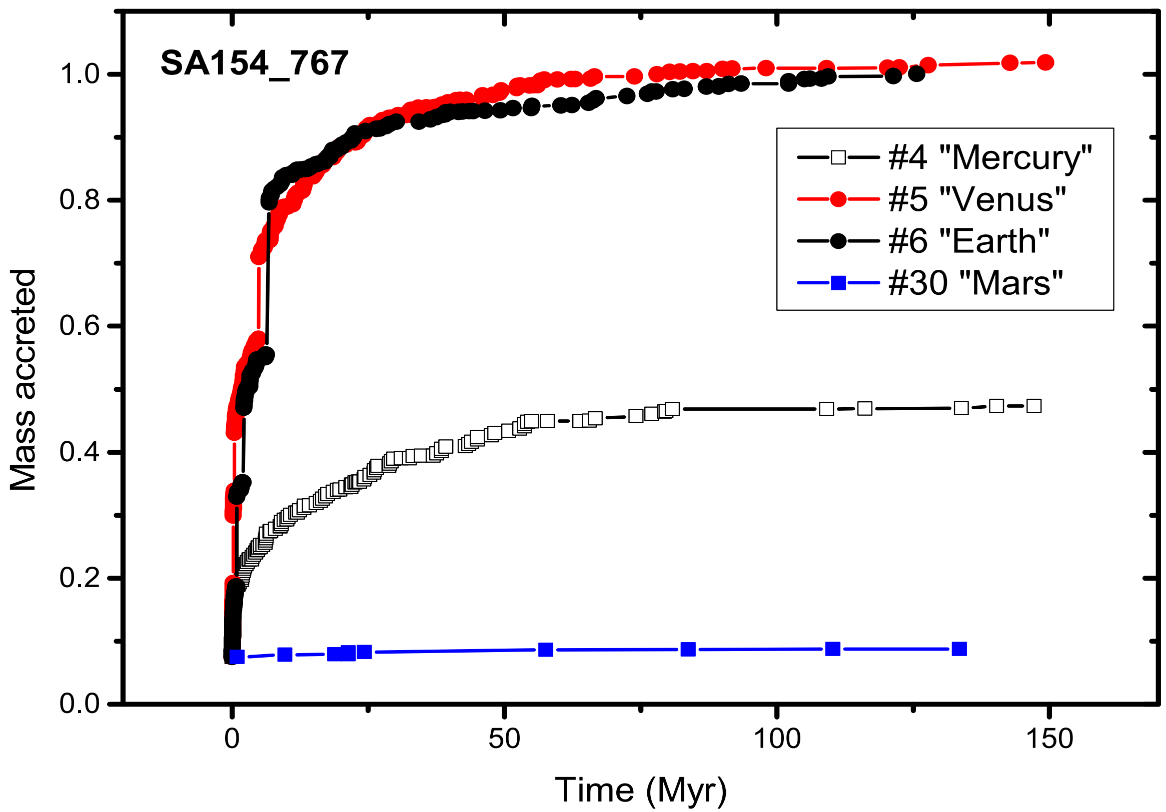


Here we consider that each accretion event (collision) results in an episode of core formation and we thus model core formation and evolving mantle and core chemistry in all the terrestrial planets simultaneously

# Model for the influence of a spin transition in ferropericlase

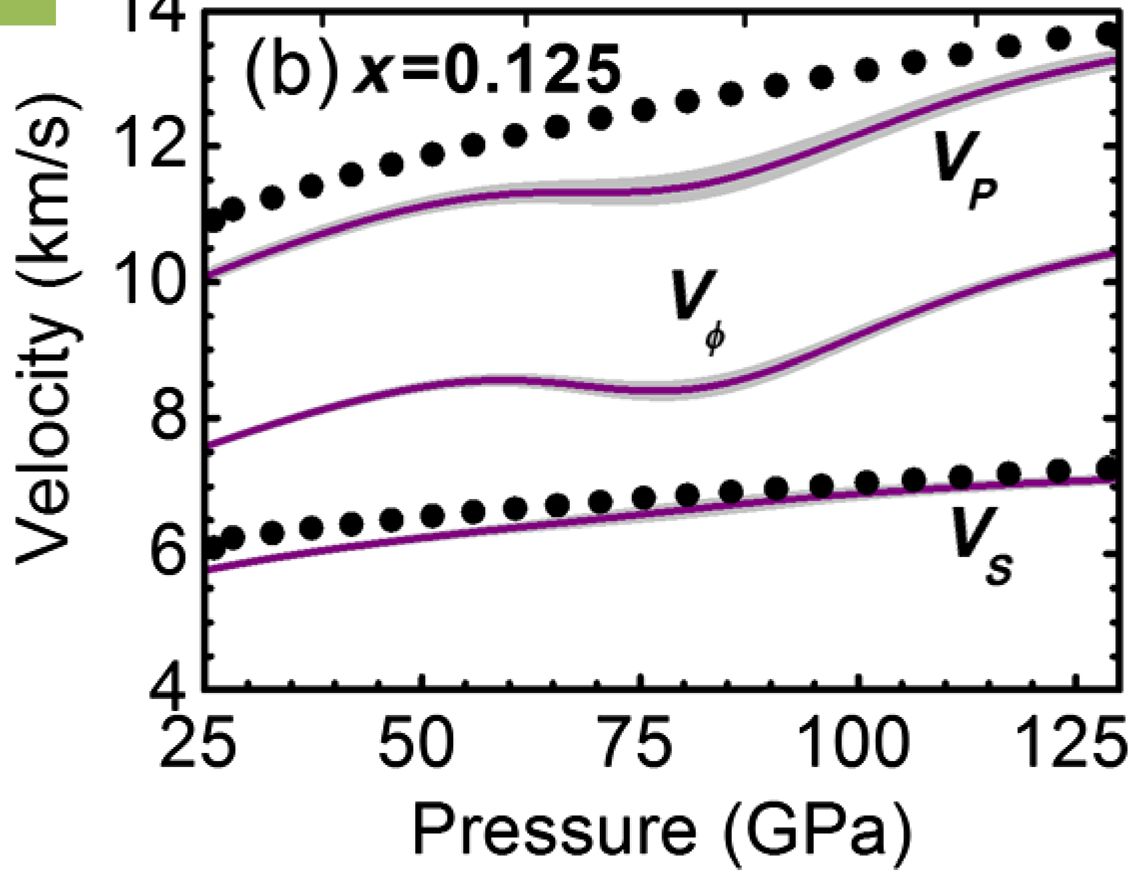


Wu et al. 2013

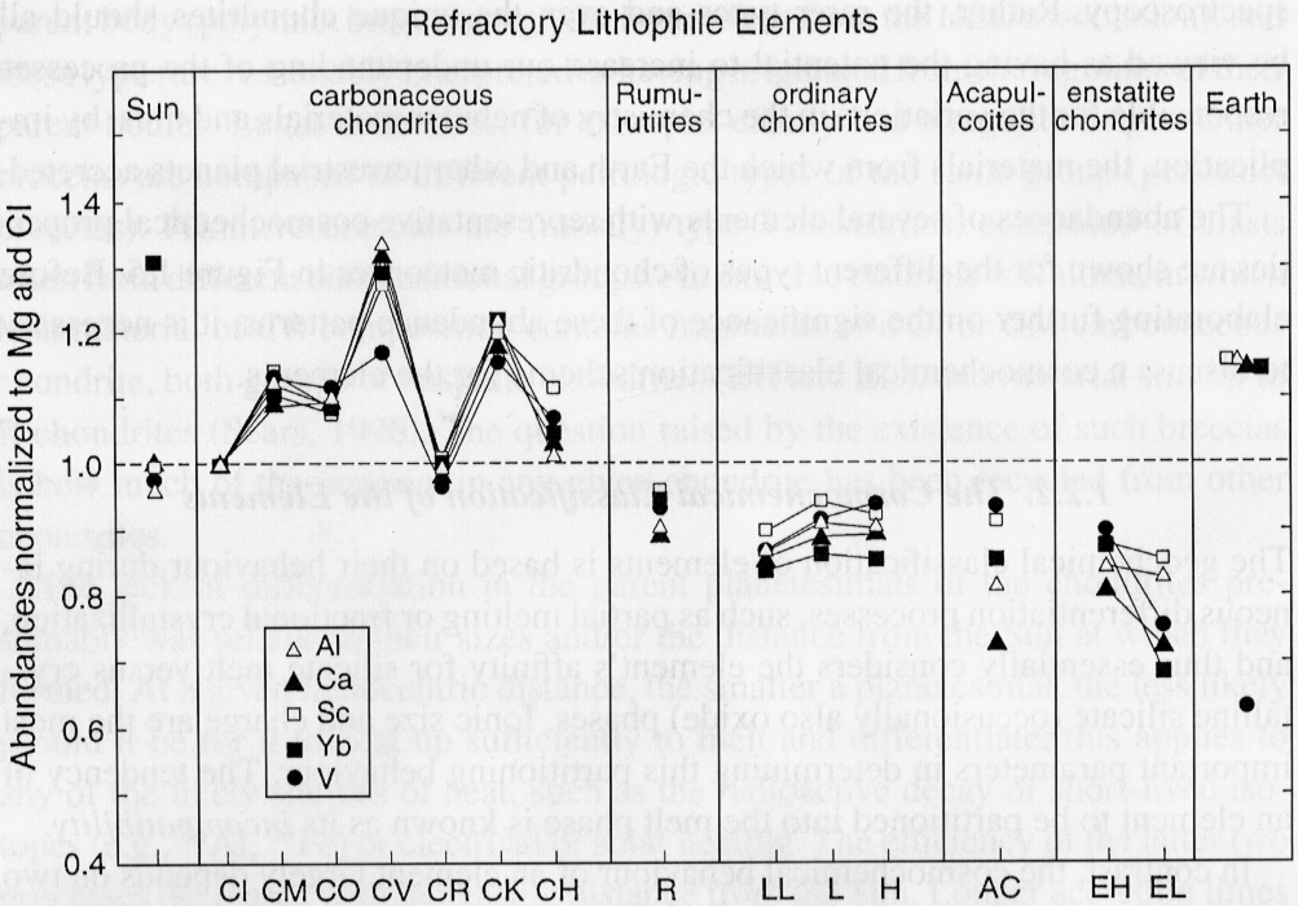
Refractory Lithophile Elements
Sun
carbonaceous chondrites
Rumu-rutiites
ordinary chondrites
Acapul-coites
enstatite chondrites
Earth
Abundances normalized to Mg and CI
1.4
1.2
1.0
0.8
0.6
0.4
Al
Ca
Sc
Yb
V
CI CM CO CV CR CK CH
R
LL L H
AC
EH EL